Revista Ibérica de Aracnología, nº **38** (30/06/2021): 163–185.
Grupo Ibérico de Aracnología (S.E.A.). ISSN: 1576 - 9518.

IBERESIA CASTILLANA (FRADE & BACELAR, 1931), REDESCRIPTION OF THE MALE, FIRST DESCRIPTION OF THE FEMALE, AND A KEY TO THE PRESENTLY KNOWN SPECIES OF GENUS *IBERESIA* (ARANEAE, NEMESIIDAE)

José Antonio Luis De La Iglesia[1*], Marta Calvo García[2],
Cristian Pertegal Pérez[3] & Rafael Molero Baltanás[4]

[1] Ctra de Pinto a San Martín de la Vega, km. 5. 28340, Valdemoro, Madrid, España. * Corresponding author: jalemys@gmail.com
[2] San Pedro, 29, 30205, Cartagena, Murcia, España. martacalvo.mininos@gmail.com
[3] Departamento de Zoología, Universidad de Córdoba, Edificio C-1, Campus de Rabanales, 14071, Córdoba, España. cristianpertegal@hotmail.es
[4] Departamento de Zoología, Universidad de Córdoba, Edificio C-1, Campus de Rabanales, 14071, Córdoba, España. ba1mobar@uco.es

Abstract: *Iberesia castillana* (Frade & Bacelar, 1931) is a trapdoor spider species described from a single male specimen collected from Ávila (Castilla y León, Spain) and kept at the Muséum National d'Histoire Naturelle", Paris. In this work the description of the male is updated, and the female is described for the first time. Although we have not been able to collect new specimens from the type locality, we have found that this species occurs south of the Central System mountain range in localities of the province of Ávila, and in more remote areas, in the provinces of Ciudad Real (Castilla La Mancha) and Córdoba (Andalusia), thus showing a much broader distribution than that suggested by the only record reported so far. Our results, that show a remarkable intraspecific variability, allowed us to rewrite and complete the key to species of the genus, which now includes the males and females of all species of *Iberesia* described so far.
Key words: Mygalomorphae, Nemesiinae, Nemesiini, trapdoor spiders, Iberian Peninsula, Spain, Ávila, Ciudad Real, Córdoba

***Iberesia castillana* (Frade & Bacelar, 1931), Araneae, Nemesiidae: redescripción del macho, primera descripción de la hembra, y una clave de las especies del género *Iberesia* conocidas hasta el momento**
Resumen: *Iberesia castillana* (Frade & Bacelar, 1931) es una especie de araña trampera descrita a partir de un único ejemplar macho de la colección Simon depositada en el Muséum National d'Histoire Naturelle", Paris. En este trabajo se actualiza la descripción del macho y se describe la hembra por vez primera. Aunque no hemos podido recolectar nuevos especímenes en la localidad típica (Ávila, Castilla y León, España), hemos encontrado esta especie en localidades próximas de la provincia de Ávila, al sur del Sistema Central, y en zonas más alejadas, en las provincias de Ciudad Real (Castilla La Mancha) y Córdoba (Andalucía), lo que demuestra que su distribución es mucho más amplia de lo que sugiere el único registro documentado hasta ahora. Estos resultados nos han permitido reelaborar la clave del género, que incluye ahora a los machos y hembras de todas las especies de *Iberesia* descritas hasta el momento.
Palabras clave: Mygalomorphae, Nemesiinae, Nemesiini, arañas tramperas, Península Ibérica, España, Ávila, Ciudad Real, Córdoba

Introduction

The trapdoor spiders of the family Nemesiidae Simon, 1889 are cryptic sedentary species that live in burrows from which they rarely emerge, except for males during the mating season (Pérez-Miles & Perafán, 2017). These facts are probably why quite a few species are known from a few specimens (Barrientos & Ferrández, 1981), often from only one of the sexes (Frade & Bacelar, 1931; Barrientos & Ferrández, 1981; Blasco, 1986a, b; Decae, 1995, 2005, 2012; Cardoso, 2000). Many of the old descriptions of these species are brief, incomplete, and poorly illustrated; furthermore, in some cases the type material was unavailable (Decae *et al.*, 2007), which considerably complicates both the assignment of specimens to already described species and the description of new taxa, given the risk of incurring synonymy. To make matters worse, the morphology of *Nemesia* and *Iberesia* genera is remarkably uniform (Decae, 2005), and it shows considerable intraspecific variation that affects even characters generally considered diagnostic (see Discussion below), further confusing the study of this group of arachnids.

Iberesia castillana (Frade & Bacelar, 1931) was described as *Nemesia castillana* from a single male collected in Ávila found in the Simon collection at the Muséum National d'Histoire Naturelle", MNHN (Frade & Bacelar, 1931). The species was later transferred to the genus *Iberesia* Decae & Cardoso, 2005, authors who completed the description of the species from the same specimen. A later record of two juveniles from Olmedo, (Valladolid, Castilla y León) by Barrientos & Gómez (2014) should be considered unreliable because this identification was based on geographic arguments rather than on morphology. Subsequent attempts to find the species in the vicinity of the type locality were unsuccessful (Mora, 2015, p. 127; Luis de la Iglesia, 2019a, p. 169).

In a new attempt to rediscover *Iberesia castillana*, in 2019 we carried out an intense sampling in different locations in the province of Ávila resulting in the collection of specimens of two syntopic species of *Nemesia* near the city of Ávila, and specimens of one species of *Nemesia* and one species of *Iberesia*, also occurring syntopically, from the south and east of Sierra de Gredos mountain range. A new study of specimens previously wrongly identified as *I. machadoi* Decae & Cardoso, 2005 (Morano, 2017, p. 105) confirmed the occurrence of this species in Las Tablas de Daimiel National Park (Ciudad Real, Castilla La Mancha). Finally, a sample of *Iberesia* specimens collected near Córdoba (Andalusia), and in Fuencaliente (Ciudad Real, Castilla La Mancha) shows great similarity and few differences with those of Gredos and Daimiel, and we believe that they are conspecific. The occurrence of *I. castillana* over a wide area

of the centre and south of the Iberian Peninsula (fig. 1) is somewhat surprising, given the lack of records since it was first described, and reflects that the Spanish nemesiid fauna has been poorly studied.

In order to compare our material with the holotype, we requested and obtained some photographs from the holotype of *Iberesia castillana* preserved at the MNHN, which allowed us to take measurements of the holotype and confirm the affiliation of the males in our sample to that species. The redescription *Iberesia castillana*, following the criteria of the recent literature on Mediterranean nemesiids, constituted the main purpose of this work. In addition, some morphologic characters show intraspecific variation, both within and between these populations, therefore a second objective was to describe such variation. Finally, an improved determination key is proposed for the species of the genus *Iberesia*.

Material and methods

Eighty-nine *Iberesia castillana* specimens from three different regions (fig. 1) collected in pitfall traps, by burrow excavation, and by manual collection have been examined in this work (Table I). The sample from Sierra de Gredos (province of Ávila, Castilla y León) includes specimens from Arenas de San Pedro (28 ♂♂, 4 ♀♀ collected in pitfalls; 3 ♀♀ captured from their nests), Mombeltrán (1 ♂ in a pitfall); and El Tiemblo (1 ♂ found dead under a stone). The sample from the province of Ciudad Real (Castilla La Mancha) consists of 8 specimens from the "Parque Nacional de las Tablas de Daimiel", PNTD, (Isla Algeciras: 5 ♂♂, 1 j: Isla del Pan: 2 ♂♂) and 1 ♂ from Fuencaliente. The sample from the Alcolea-Córdoba area includes 7 ♂♂, 13 ♀♀, 2 jj, and 2 larvae from Alcolea (Córdoba, Andalusia), 15 ♂♂ from Córdoba, 3 ♀♀, 1 j from El Higuerón (Córdoba). The specimens from the PNTD are part of the project to study the arachnofauna of the National Park (Morano, 2017); some specimens of the Alcolea-Córdoba sample belong to the funds of the "Departamento de Zoología de la Universidad de Córdoba", UCO; the remaining specimens belong to the authors' collections except for those that have been donated to the "Museo Nacional de Ciencias Naturales" (MNCN), and MNHN (see Table I).

The specimens collected in pitfall traps were cleaned with water and preserved in 70% ethanol with a few drops of glycerine; those captured alive were killed and preserved in 70% ethanol. They were examined in containers with 70% ethanol under a Unitron Z850 trinocular stereomicroscope and with a Euromex MIC0800 microscope. Photographs were made with an AmScope MU10000 camera attached to each microscope at × 10 and × 20 (body and appendages, precision 0.1 mm), × 30, × 40 and × 50 (palpal tibial rake, eye formation, spinnerets, epiandrous spigots, bulbs and spermathecae, precision 0.01 mm). Measurements were taken with the aid of ToupView software measurement tools calibrated with a stage micrometre (precision 0.01 mm); they are given in millimetres and follow the methodology described in the works by Decae (Decae, 2005: fig. 2−8; Decae & Huber, 2017: fig. 2) with some modifications explained in figure 2. Some photographs have been processed using the "Stitch" and "EDF" (extended depth of focus) tools of ToupView.

Twenty-one females were dissected to extract the spermathecae for study; some of them were examined on small plates in 70% ethanol after removing the surrounding tissue with fine needles; the rest were treated with 10% KOH solution and mounted on slides with "Tendeiro liquid" as a mounting medium (Molero-Baltanás *et al.*, 2000). Some premoult or recently moulted females allowed the study of spermathecae before and after moult.

Additional material: the study includes two specimens of *Iberesia arturica* Calvo, 2019, five specimens of *Iberesia machadoi* and four of *Iberesia valdemoriana* Luis de la Iglesia, 2019a for comparative purposes.

Table I includes the list of the specimens used in this work, as well as other data including georeferencing, when available. The geographic coordinates were obtained using a GPS system (datum WGS84).

Terminology follows the terms and ratios of general use in the recent literature on Mediterranean nemesiids (Decae, 2005; Decae & Cardoso, 2005; Decae et al., 2007; Decae & Huber, 2017; Luis de la Iglesia, 2019a). New ratios have been defined and are described in Figure 2. We include some data on male epiandrous spigots or *epiandrous fusillae* (Zonstein, 2009). The genital spigots (Fage & Machado, 1951; Machado, 1951) or epiandrous glands (Marples, 1967), are part of the epigastric apparatus (Lopez & Emerit, 1988) or epiandrous apparatus (Michalik & Ulh, 2005). It is formed by silk glands, some of them ended in spigots, located in the anterior margin of male epigastric furrow of many groups of spiders, and are involved in the production of sperm web (Ferretti *et al.*, 2017). In mygalomorph spiders, the epigastric area is almost completely occupied by many isolated epiandrous spigots (López & Emerit, 1988) grouped in a semicircular or crescent field (Ferretti *et al.*, 2016) (fig. 2A). Setiform spigots, with an inflated base and tapered tip, are placed in a wide round socket (López & Emerit, 1988; Ferretti *et al.*, 2017) (fig. 2B). In some Mygalomorphae, clear interspecific differences have been found in the diameter of the sockets and in the width of the base of the spigots (Ferretti *et al.*, 2017). In our material we have found differences in the density of spigots of *I. machadoi* and *I. castillana* (see Discussion). Epiandrous spigot density is calculated as number of spigots per surface area of the epiandrous apparatus field; the latter was measured by calculating the area of the polygon whose sides touch the outermost spigots of the field; its length is the distance between the epigastric furrow and the farthest spigot rostrally (fig. 2A).

Abbreviations: ALE = anterior lateral eye, AME = anterior median eye (cornea), AME−AME = anterior median eyes interspace (between corneas), AMEi = inner diameter of anterior median eye ("pupil"), AR = anterior eye row, BL = body length (spinnerets not included), Bu = bulb height, Ca = caput length, Ch = caput height, Cl = carapace length, Cly = clypeus height, Cw = carapace width, Cy = cymbium, Dh = spermatheca duct height (granular part), Dw = spermatheca duct width, EFA = epiandrous apparatus field area, EFL = epiandrous apparatus field length, EL = eye group length, Em = embolus height, ESD = density of epiandrous spigots, ESN = number of epiandrous spigots, Fe = femur length, Ll = labium length, Lo = proximal bulb lobe height, Lw = labium width, Me = metatarsus length, Ml = maxilla length, Mw = maxilla width, Pa = patella length, PLE = posterior lateral eye, PLS = posterior lateral spinnerets, PLSb, PLSm, PLSa = basal, median and apical segments of PLS, PME = posterior median eye, PMS = posterior median spinnerets, POP = periocular pigmentation, PR = posterior eye row, PSP = prolateral spines on patellae,

Rh = spermatheca receptacle height, RSP = retrolateral spines on patellae, Rw = spermatheca receptacle width, Se = distance between spermathecae, external, Sg = spermatheca granular part height, Sh = spermatheca height, Si = distance between spermathecae, internal, Ss = spermatheca smooth, non-granular part height, Stl = sternum length, Stw = sternum width, Ta = tarsus length, Th = thorax height, Ti = tibia length, Tiw = palpal tibia width.

Ratios: ALE/PLE = diameter anterior lateral eye / posterior lateral eye, AR/EL = anterior eye row width / eye group length, AR/PR = anterior eye row width / posterior eye row width, Bu/Em = bulb length / embolus length, C(l/w) = carapace length / carapace width, Ch/Th = caput height / thorax height, Cly/ALE = clypeus height / diameter anterior lateral eye, Cly/EL = clypeus height / eye group length, Dh/Rh = spermatheca duct height / receptacle height, Em/Lo = embolus height / proximal lobe height, L(l/w) = labium length / labium width, M(l/w) = maxilla length / maxilla width, Rw/Dw = spermatheca receptacle width / duct width, Se/Dw = distance between spermathecae (external) / duct width, S(g/h) = spermatheca granular part height / spermatheca height, S(g/s) = spermatheca granular part height / spermatheca smooth, non-granular part height, Si/Dw = distance between spermathecae (internal) / duct width, St(l/w) = sternum length / sternum width, Ti(l/w) = palpal tibia length / palpal tibia width.

Institutions: MNCN: Museo Nacional de Ciencias Naturales, Madrid; MNHN: Museum National d'Histoire Naturelle, Paris; PNTD: Parque Nacional de las Tablas de Daimiel, Ciudad Real; UCO: Departamento de Zoología de la Universidad de Córdoba.

Taxonomy

Family NEMESIIDAE Simon, 1889

Genus ***Iberesia*** Decae & Cardoso, 2005

***Iberesia castillana* (Frade & Bacelar, 1931)**

Fig. 2, 3A, 4A, 5A, 6B, 7B, 8F, 9–29, 31–32, 34.

Nemesia castillana: Frade & Bacelar, 1931: pp. 224–226, fig. 5–6 (♂).

Iberesia castillana: Decae & Cardoso, 2005: p. 9, fig. 14 (♂); Le Peru, 2011: p. 75, fig. 48 (♂); Barrientos & Gómez, 2014, p. 105 (j); Zonstein, 2016: fig. 21, 26 (♂); Luis de la Iglesia, 2019a: fig. 2A, C (♂).

DIAGNOSIS. *Iberesia castillana* differs from *I. machadoi* and *I. arturica* in its smaller body size; furthermore, males of *Iberesia castillana* differ from all other congeneric males in the shape of the palpal tibia (narrow in *I. castillana*, thickened in the other species; fig. 3). They differ from *I. brauni* (Koch, 1882), *I. barbara* (Lucas, 1846), *I. valdemoriana* and *I. arturica* in the shape of the sexual organ (embolus slightly sigmoid in *I. castillana* but curved in the other species; fig. 4). Females of *Iberesia castillana* differ from all other *Iberesia* species by their spermathecae with barrel-shaped ducts (fig. 8).

KEY TO SPECIES

Males

1a. Palpal tibia slightly dilated at its base, more than twice longer than wide (fig. 3A). Bulb: proximal lobe shorter than the embolus; narrow embolus base; embolus tip sigmoid, smooth or with up to 3 distal minute denticles on its convex side (fig. 4A). Sigilla barely visible, close to the margin of sternum; the third pair at most one diameter away from the sternum border (fig. 5A). Medium-sized species (BL < 16 mm). Central Spain mainland..... ..... *Iberesia castillana*

1b. Papal tibia dilated at its base, less than twice longer than wide (fig. 3B); large or medium-sized species 2

2a. Embolus tip sigmoid or curved, wearing some prominent subdistal denticles on its convex side (fig. 4B–C). Large sized species (BL = 17–22 mm)..... 3

2b. Embolus tip clearly curved, with some tiny subdistal denticles on its concave side (fig. 4D–F). Medium sized species (BL = 12–15 mm) 4

3a. Sigilla clearly visible, separated from the margin of the sternum; the third pair at least two diameters from sternum border (fig. 5B). Embolus: narrow base, tapering distally; embolus tip sigmoid, with 2 prominent distal denticles on its convex side (fig. 4B). BL = 17–18 mm. West and southwest of the Iberian Peninsula .... *I. machadoi*

3b Sigilla close to the margin of the sternum; the third pair about one diameter from sternum border (fig. 5A). Embolus: wide base, abruptly narrowed distally; embolus tip clearly curved, with 2–3 prominent distal denticles on its convex side (fig. 4C). BL = 17–22 mm. Southeast of the Iberian Peninsula ..... *I. arturica*

4a. Bulb: embolus longer than proximal lobe. Embolus: narrow base; embolus tip with 2–4 denticles (fig. 4F). Patellae I–IV usually with 0–1 prolateral spines. Central and southeast Spain mainland ..... *I. valdemoriana*

4b. Bulb: proximal lobe almost the same length as the embolus or a bit longer. Embolus: wider base (fig. 4D–E). Patellae I–IV usually with 1–2 prolateral spines 5

5a. Bulb: embolus slightly longer than proximal lobe. Embolus: base of intermediate thickness; embolus tip with 2 barely visible denticles (fig. 4E). Mediterranean coast of Morocco and Algeria (see note below)..... *I. barbara*

5b. Bulb: embolus subequal in length to proximal lobe. Embolus: base slightly wider; embolus tip with 2–3 denticles, sometimes barely protruding (fig. 4D; bulb remarkably similar and difficult to distinguish to the former one). Eastern Spain mainland and Balearic Islands ..... *I. brauni*

Females

1a. Tripartite or bipartite spermathecae. Large-sized species (BL = 20–34 mm)..... 2

1b. Bipartite mushroom-shaped spermathecae (fig. 8B–F). Sigilla close to the margin of sternum; the third pair at most one diameter away from the sternum border (fig. 6B). Medium-sized species (BL < 25 mm) 3

2a. Tripartite spermathecae with broad basal part and narrow intermediate collar connected to a dome-shaped distal receptacle (fig. 8A). Sigilla separated from the margin of the sternum; the third pair at least two diameters from sternum border (fig. 6A). Spineless patellae. Eye group more than twice longer than wide, AR = PR, ALE ≤ PLE. Clypeus clearly higher than ALE, similar in height to EL (fig. 7A). BL = 20–29 mm. West and Southwest of the Iberian Peninsula ..... *Iberesia machadoi*

2b. Bipartite spermathecae; clearly divergent ducts; narrow basal part (fig. 8B). Sigilla close to the margin of sternum; the third pair about one diameter away from the sternum border (fig. 6B). Palpal and leg I–III patellae

usually with 1 prolateral spine. Eye group twice longer than wide, AR < PR, ALE > PLE. Clypeus lower than ALE, half of EL (fig. 7B). BL = 24–34 mm. Southeast of the Iberian Peninsula ..... *I. arturica*

3a. Spermathecae: tube-shaped ducts; receptacles clearly wider than ducts (fig. 8C, E) 4

3b. Spermathecae: barrel-shaped ducts; receptacles similar in width to ducts (fig. 8D, F) 5

4a. Short spermathecae; part of the duct covered with granular tissue of similar height to the receptacle (fig. 8C). Eastern Spain mainland and Balearic Islands ... *I. brauni*

4b. Long spermathecae; part of the duct covered with granular tissue higher than the receptacle (fig. 8E). Central and southeast Spain mainland ..... *I. valdemoriana*

5a. Spermathecae: smooth non-granular proximal ducts wider than receptacles (fig. 8D), external distance long (Se > 1.00 mm). Clypeus higher than ALE (Cly/ALE > 1.00) (see note) ..... *I. barbara*

5b. Spermathecae: smooth non-granular proximal ducts narrower than receptacles (fig. 8F), external distance short (Se ≈ 0.76 mm). Clypeus shorter than ALE (Cly/ALE < 0.80, fig. 7B) ..... *I. castillana*

Note: In a study of the nemesiid fauna of the province of Cádiz we have not been able to find any male assignable to *I. barbara* (Luis de la Iglesia, Pertegal, Calvo, in preparation). However, we have found females with sexual organs similar to those of *I. barbara*, but with other significant differences. This suggests that populations from Cádiz likely correspond to a different species, not yet described, and that the affiliation to *I. barbara* of the specimen collected in Zahara de los Atunes (Cádiz) cited in a previous paper (Luis de la Iglesia, 2019a) should be provisionally considered as unconfirmed. Consequently, we have not used the description of that specimen in the elaboration of this key.

DESCRIPTION OF MALE (specimen #MNCN 20.02/19859, Table I)

Habitus: nemesiid of medium size (BL = 13.9), long, thin appendages and slender abdomen (fig. 9B). Colour of living specimen: carapace covered with whitish pubescence; dark brown chelicerae with light pubescent bands; abdomen with brown blotches on light background; legs light brown, femurs dorsally dark (fig. 9A). Colour in alcohol: carapace with dark brown caput and lighter thin marginal band, rostral margin darker; thorax orange-ochre, slightly darker spot with radial pattern centred on fovea (fig. 9B, 10A), whitish pubescence on carapace and chelicerae (fig. 11). POP dark brown (fig. 12), 3-spot pattern, i.e., central stripe surrounding AME, plus two darker lateral strips between inner margin of group ALE-PLE-PME. Chelicerae not contrasting with caput with slightly light longitudinal band. Dorsal abdomen with six brown chevrons (partially faded) on ochre background (fig. 9B, 10A). Uniform yellow sternum and coxae, brown labium with clear anterior border; ochre maxillae (fig. 13A–B); shiny, dark red cheliceral fangs (fig. 14A–B). Abdomen ventrally yellow-cream, posterior lung plates a bit more intensely coloured; two small greyish maculae on inner border of posterior lung plates (fig. 13A); spinnerets, same colour as the abdomen (fig. 15A–B). Dorsal femora ochre with dark longitudinal bands, dorsal cymbium tanned (fig. 2C, 16), rest of appendages, including tarsi, light yellow.

Carapace oval, C(l/w) = 1.20, notched at pedicel insertion, covered with thick pubescence, denser in cephalic area; scattered black bristles in thoracic area, more abundant caudally (fig. 10A). Thick fringe setae recurved over coxae I–II and coxa III, procurved between coxae II−III and behind coxa III. Caput slightly elevated (fig. 11), crest zone indistinct with three rows of crest setae; central row with thicker, longer setae, lateral rows with smaller setae. Recurved fovea, with central longitudinal groove (fig. 10A). Eye formation twice as wide as long (fig. 12); AR clearly procurved, same width as PR, latter slightly procurved. ALE clearly larger than PLE (ALE/PLE = 1.43); clypeus lower than ALE (Cly/ALE = 0.61).

Sternum longer than wide, angular, covered with short, strong black setae; broad, smooth labiosternal junction; labiosternal sigilla not apparent; sternal sigilla barely visible, anterior small, round, adjacent to margin, median slightly distant from margin, posterior sigilla larger, slightly oval, one diameter away from margin (fig. 13A–B). Labium short, rostrally notched, 2.5 times wider than long. Maxillae subrectangular, blunt anterior process; single curved row with 5 setiform cuspules; sparse orange maxillary scopulae (fig. 13B, 14A). Chelicerae dorsally with internal band of stout bristles, short spines rostrally; rastellum with five short, strong spines, interspersed with numerous thick bristles. Cheliceral furrow with promarginal row of six unequal teeth; those occupying positions 5 and 2 larger (counting from distal to proximal); row of 20 (23) tiny mesobasal denticles, largest rostrally (fig. 14A); prolateral fang keel irregularly notched (fig. 14B).

Abdomen ventrally covered with setae, longer and denser in caudal area (fig. 13A). Epigastric apparatus made up of 22 epiandrous spigots interspersed with short hairs, grouped in small crescent close to epigastric furrow, bordered laterally and anteriorly by long curved black setae (fig. 2A, 13C). Spinnerets: basal segment 2.2 times longer than middle segment; short distal domed segment. Scattered aciniform spigots in ventral area of basal and middle segments (fig. 15A); apical area of distal segment with few scattered spigots and ring of 5–6 larger spigots surrounding single central macro-spigot (fig. 15B).

Appendages. Patellar formulae (according to Decae *et al.*, 2007; abbreviated notation): PSP: p=1-1; I=2-2; II=2-2; III=2-2; IV=0-1; RSP: p=0-0; I=1-0; II=0-0; III=1-1; IV=0-1. Leg IV formula: Me>Fe>Ti. Leg formula: 4 1 2 3.

Palp: femur slightly curved inward with faintly marked dorsal ridges; spines, dorsal 1-1-2, prodorsal 1; ventrally, marginal series of long spines and spiniform setae; patellae, short; tibia with slightly thickened base (ratio Ti(l/w) = 2.30; fig. 2C, 16). Prodorsal tibial rake with two rows of thick spines, prolateral larger. Spine alignment 3+0+1, i.e., first apical row with 3 parallel spines, second row with no spine (compared to other males), and third row with 1 larger spine (fig. 17B).

Legs covered with black hairs on dorsal, pro, and retrolateral sides, denser on femora; latter with two faded dorsal ridges. Clasper: tibia I distally widened, short conical, proventral spur, mega-spine slightly curved upwards and inwards, not too strong (fig. 18A); clasper field formed by short, pointed spikes covering slightly thickened distal two thirds of metatarsus I (fig. 18B). Bipectinate paired tarsal claws with uneven series of 9–13 combs; unpaired claw short, curved, unarmed. Spination: femora with series of up to 6 dorsal spines plus 2–3 apical ones, 2–4 pro, and 3–4 retrolateral spines; ventrally two marginal series of long spines and spiniform setae. Patellae: see patellar formulae;

patella III displays dorsally 2–5 spines and proximal groups of spiniform setae. Tibiae I–II with 3 pro, and 3 retrolateral spines, and three pairs of ventral spines (proventral apical spine modified into a spur as described above); tibia III dorsally with 2 basal plus 1 median spines, and series of 3 pro, and 3 retrolateral spines; apical spine, corresponding to female's super-spine (see below), somewhat stronger, inserted into thicker socket; tibiae IV with 1 basal pair plus 2 dorsal spines, series of 4 pro, and 3 retrolateral spines; tibiae III–IV with three pairs of ventral spines with uneven insertion points (basal, medial and distal, sometimes 3 distal spines). Metatarsi I–II with subdistal and apical pairs of spines, and series of 3–4 pro, 4 retrolateral, 2–3 ventral apical spines; metatarsi III, dorsally 3 pairs of spines; series of 3–4 pro, 3 retrolateral spines, ventrally 2-2-3; metatarsi IV, dorsally 1-1-1-2, series of 4 pro, 3 retrolateral, ventrally, 1-2-2-2-4. On metatarsi and tibiae, spines of spine pairs are uneven, sometimes lacking, being difficult to choose in which side they lay, making description of spine patterns inaccurate. Tarsi with single or double series of short spines. Scopulae ventrally sparse in distal half of tarsi I–II, even less dense in distalmost part of metatarsi I–II; missing elsewhere. Trichobothria: two rows of 6–9 each on tibiae, one irregular row of 11−14 on metatarsi, and in zigzag row of 12−14 on tarsi, 10 on cymbium.

Palpal organ (fig. 2C, E, 4A, 16, 19A–B): pyriform bulb with short, round proximal lobe, extending into long, narrow embolus tapering distally (Bu/Em = 1.69; Em/Lo = 1.45); shallow longitudinal groove on ventral side of embolus (fig. 19A); embolus distally sigmoid, garnished with 2 subdistal small denticles on convex side (fig. 19B).

VARIATION. Marked intraspecific variation affecting many characters, including coloration, eye formation, number of cuspules, serration of fang keel, patellar formulae, palpal tibial rake settings, spination, and embolic denticles. Cephalothorax colour varies from *bicolour pattern* described above –i.e., dark brown caput and chelicerae; orange ochre thorax, fig. 9B, 10A– to *dark pattern* (caput and thorax indistinctly dark, not contrasting, fig. 10B); specimens from Gredos show full range between these two patterns; those from Daimiel and most of Alcolea-Córdoba show bicolour pattern; finally, some individuals in Alcolea-Córdoba sample show *light pattern* (fig. 15C) maybe due to fading in the preservation medium. Carapace pubescence varies from whitish to yellowish, and from sparse to dense; no population differences observed. POP varies form 1-spot pattern to 3-spot pattern (*sensu* Luis de la Iglesia, 2019a, p. 164). Dorsal abdomen design varies from chevron pattern to tangled pattern. Posterior lung plates more intensely coloured in some specimens, especially in Alcolea-Córdoba sample.

Eye group with ALE clearly larger than PLE in Gredos sample (ALE/PLE = 1.31), slightly larger in Alcolea-Córdoba sample (ALE/PLE = 1.11), intermediate in Daimiel sample (ALE/PLE = 1.23). Clypeus lower than ALE in all specimens, ratio Cly/ALE lower in Gredos sample (0.67), higher in Alcolea-Córdoba sample (0.81), and intermediate in Daimiel sample (0.72). Prolateral fang keel ranging from irregularly notched to distinctly serrated; fang serrations visible from the earliest larval stages. Number of maxillary cuspules ranging from 3–7 setiform cuspules. Fovea central groove small or indistinct in some specimens.

Patellar formulae: PSPvar: p=1(0–2); I=1(2–3); II=2(1); III=2(0–3); IV=1(0–3); RSPvar: p=0; I=1(0); II=0(1); III=1(0–2); IV=1(0). Leg IV formula: Me>Fe>Ti = 74%; Me≈Fe >Ti = 17%; Fe>Me>Ti = 9%.

Spine settings in prodorsal tibial rake strongly variable (fig. 17A–J). Spine number and thickness vary greatly both between individual and in both sides of the same specimen; tarsi occasionally bearing solitary long spines in different positions. Embolus showing 0–3 subdistal small denticles on convex side (often hardly visible as tiny granules; fig. 19B, D, F).

In contrast, cheliceral teeth number remains very constant: 91% males have 6 teeth, rarely, 5, 7 or 8; similarly, all males studied show a single macro-spigot in distal segment of spinnerets.

We have also found some teratological specimens including three males with unusually narrow sternum, St(l/w) = 1.69–1.97 (fig. 20A), two specimens with double macro-spines on the spur of tibia I (fig. 20B); and a male with posterior lung plates stained dark brown (fig. 20C).

Morphometric variation (n = 60): measurements (in mm, unless otherwise indicated) given as mean value and range of variation, in parentheses; major differences between samples from Gredos, Daimiel or Alcolea-Córdoba indicated in square brackets preceded by G, D, or A, respectively. BL = 13.0 (9.6–15.8). Cephalothorax: Cl = 5.3 (3.9–6.0); Cw = 4.5 (3.6–5.0); C(l/w) = 1.18 (1.00–1.30); Ca = 3.3 (2.5–3.8); Ch/Th = 1.34 (1.24–1.41); Stl = 2.9 (2.5–3.3); Stw = 2.1 (1.8–2.5); St(l/w) = 1.36 (1.28–1.45); Ll = 0.4 (0.3–0.5); Lw = 0.9 (0.7–1.1); L(l/w) = 0.40 (0.33–0.47); Ml = 1.9 (1.5–2.1); Mw = 1.0 (0.8–1.2); M(l/w) = 1.82 (1.55–2.00). Eye group: EL = 0.52 (0.42–0.61); AR = 1.00 (0.82–1.17); PR = 1.00 (0.81–1.16); AR/PR = 0.99 (0.94–1.03); AR/EL = 1.91 (1.72–2.16), D [2.01 (1.92–2.16)]; AME=0.24 (0.20–0.29); AMEi = 0.16 (0.11–0.21); AME−AME = 0.07 (0.05–0.12); ALE = 0.31 (0.24–0.39); PLE = 0.25 (0.20–0.32); ALE/PLE = 1.23 (0.89–1.43), G [1.31 (1.07–1.43)], A [1.11 (0.89–1.32)]; PME = 0.18 (0.14–0.23); Cly = 0.22 (0.16–0.30); Cly/ALE = 0.72 (0.53–1.03); Cly/EL = 0.43 (0.35–0.59). Epigastric Apparatus: ESN (spigots) = 27 (18–43); ESD (spigots/mm^2) = 107 (71–144). Spinnerets (only fully extended spinnerets were measured): PLS = 1.34 (1.15–1.54) {PLSb = 0.78 (0.64–0.88), PLSm = 0.36 (0.26–0.45); PLSa = 0.19 (0.13–0.25)}; PLSa macro-spigot number = 1 in all specimens. Appendages: palp = 8.0 (6.5–8.8) {Fe = 3.0 (2.5–3.3), Pa = 1.6 (1.3–1.8), Ti = 2.3 (1.8–2.6), Cy = 1.1 (0.9–1.2), Tiw = 1.0 (0.8–1.1), Ti(l/w) = 2.30 (2.13–2.51)}; leg I = 16.5 (14.6–18.5) {(Fe = 4.7 (4.2–5.3), Pa = 2.5 (2.2–2.9), Ti = 3.3 (2.9–3.6), Me = 3.3 (2.8–3.8), Ta = 2.7 (2.3–3.0)}; leg II = 16.2 (14.1–18.2) {(Fe = 4.5 (4.0–5.1), Pa = 2.2 (1.9–2.6), Ti = 3.3 (2.9–3.6), Me = 3.6 (3.0–4.2), Ta = 2.6 (2.1–2.9)}; leg III = 15.7 (12.5–17.8) {(Fe = 4.0 (3.2–4.6), Pa = 2.0 (1.6–2.4), Ti = 3.0 (2.3–3.4), Me = 4.0 (3.2–4.6), Ta = 2.6 (2.2–3.0)}; leg IV = 20.0 (16.1–23.0) {(Fe = 5.0 (4.0–5.7), Pa = 2.4 (1.9–2.9), Ti = 4.7 (3.6–5.3), Me = 5.1 (4.0–5.8), Ta = 2.7 (2.3–3.3)}. Palpal organ: Bu = 1.37 (1.12–1.55), Em = 0.81 (0.67–0.91), Bu/Em = 1.69 (1.59–1.79), Em/Lo = 1.45 (1.27–1.68).

Holotype measurements (from photographs courtesy of MNHN): BL = 13.0. Cephalothorax: Cl = 5.8; Cw = 4.8; C(l/w) = 1.22; Ca = 3.8; Stl = 3.3; Stw = 2.4; St(l/w) = 1.37; Ll = 0.5; Lw = 1.1; L(l/w) = 0.46. Eye group: EL = 0.62; AR = 1.11; PR = 1.12; AR/PR = 0.99; AR/EL = 1.79; AME = 0.29; AMEi = 0.20; AME−AME = 0.08; ALE = 0.36; PLE = 0.34; ALE/PLE = 1.06; PME = 0.20; Cly = 0.26; Cly/ALE

= 0.72; Cly/EL = 0.42. PSP: p=1-1; I=2-2; II=2-2; III=1-1; IV=1-1; RSP: p=0-0; I=1-1; II=0-0; III=1-1; IV=0-0. Palp: 8.9 {Fe = 3.4, Pa = 1.7, Ti = 2.6, Cy = 1.2, Tiw = 1.1, Ti(l/w) = 2.49}.

DESCRIPTION OF FEMALE (specimen #MNCN 20.02/19861, Table I)

Habitus: medium-sized, robust body, larger than males (BL = 21.2); short, stout appendages. Colour of living specimen: carapace dark brown, shiny, caput and chelicerae dark; greyish brown abdomen with dark marks reminiscent of chevrons; light yellow appendages but dark tarsi of palps and legs I-III (fig. 21A–B). Colour of preserved specimen: caput dark olive brown, light areas on sides of ocular tubercle, darker backwards; caput margins, rostral clypeus, and crest area darker, slightly clear central band on crest area; thorax dull yellow-ochre, fovea, carapace margins, and caudal zones darker; short sparse whitish pubescence towards anterior caput (fig. 22A). Pigmentation forming small dark patches on paler background. POP blackish, 3-spot pattern (fig. 24A). Sternum and coxae ochre-orange; labiosternal junction and posterior labium brown-orange, labium anteriorly yellow; maxillae darker than sternum with reddish internal scopula (fig. 25–26). Chelicerae dorsally brown, darker than caput, with lateral bands of stout black bristles opening rostrally; ventrally orange reddish; deep red fangs (fig. 27). Palps and legs yellow, dorsally like thorax; tarsi of palps and legs I-III darkened, IV yellow. Dorsal abdomen with greyish brown tangled design (fig. 22A) on yellowish background; ventrally greyish yellow with numerous black setae (fig. 25); grey maculae next to inner edge of posterior lung plates (fig. 25); spinnerets same colour as abdomen (fig. 25, 28).

Carapace elongated, slightly wavy lateral margins (fig. 22A); caput sharply elevated (Ch/Th = 2.71; fig. 23); distinct crest area, delimited by some short setae; crest setae as in male. Thorax caudally with some weak erect black setae; fovea slightly recurved. Eye formation almost twice as wide as long, AR slightly wider than PR; rest of eye group and clypeus as in male (fig. 24A). Sternum and labium as in male, maxillae shorter and wider than in male (fig. 25–26); cuspules arranged in row of 5–6 conical, thick, blunt thorns together with some setae resembling male cuspules (fig. 26–27). Chelicerae with six thick, unsharpened promarginal teeth, 5th and 2nd largest; up to 20 mesobasal denticles arranged as in male; fang keel finely notched (fig. 27).

Abdomen as in figures 22A (dorsal), 25 (ventral). Spinnerets: as in male; spigot fields in internal distal portion of basal segment, and internal part of medial segment (fig. 28A); three central macro-spigots surrounded by rings of large spigots on distal domed segment (fig. 28B).

Appendages: leg formula: 4 1 2 3; leg IV formula: Fe>Ti>Me; patellar formulae: all patellae spineless. Palp elongated, palpal tarsal claw with 2–3 prolateral basal combs difficult to see. Legs short and sturdy; leg tarsal claws bipectinate, combs confined to basal third; short hooked unpaired claw. Spination: palp, spiniform setae in femora arranged like male spines; tibiae, ventrally 2-2-3, central distal spine weaker; tarsi with basal pair of spines, series of 6–8 pairs of short spines, closer together distally. Legs lacking dorsal spines, femora with spiniform setae as in palp; patellae lacking spines, those of legs III–IV with prodorsal group of thick bristles. Tibiae I–II with line of 3 weak retroventral spines; metatarsi I–II, 2-1-3 short spines (basal spines very uneven; central apical spine weaker); tibia III, subapical retrolateral super-spine, short, thick, curved upward (sometimes absent); tibia IV lacking pro and retrolateral spines; ventrally, tibiae III–IV as in palp, spines often like spiniform setae, sometimes missing. Metatarsus III, prolateral line 0-1-1, retrolateral line 1-0-1 (subbasal spine like super-spine of tibia III, sometimes absent); ventrally 3 strong distal spines (namely, distal corona of 5 spines); metatarsus IV, prolateral medial spine, retrodorsal 1-0-1 line; distal corona of 5 spines; ventral surface of metatarsi III–IV with plenty of spiniform setae; retroventral distal preening comb on metatarsi IV. Tarsi III–IV ventrally with numerous spiniform setae, denser distally. Scopulae: divided on palpal tarsi (heavily dense laterally, dense ventrally); sparse on distal tibiae; dense in tarsi I–II and metatarsi I, moderately dense in distal metatarsi II; absent elsewhere. Trichobothria: distributed as in male; number increases with size.

Spermathecae: bipartite (according to Decae & Cardoso, 2005), mushroom-shaped; barrel-shaped ducts, almost parallel, slightly narrower than receptacles; somewhat flattened globular receptacles. Granular tissue profusely covering distal two-thirds of ducts and distal receptacles; proximal part of ducts smooth, devoid of granular tissue (fig. 29B).

VARIATION. Females show much less intraspecific variation than males; variation affects dorsal abdomen pattern (tangled to chevron-like design; fig. 22A–B), POP (3-spot –fig. 24A–B– or 4-spot patterns), number of cuspules (ranging from 3 to 8), serration of fang keel (mainly irregularly notched, less frequently smooth); maculae next to inner edge of posterior lung plates (grey, very faint or missing). Separation between spermathecae show population variation: greater in Gredos sample (fig. 2D, 8F, 29A–C) than in Alcolea-Córdoba sample (fig. 29D–F; see measurements below). As in males, number of cheliceral teeth remain very constant (6 in 96.2% of chelicerae).

Morphometric variation (n = 23, only adult females measuring Cw ≥ 4.0 mm included): measurements (in mm, unless otherwise indicated) given as mean value and range of variation, in parentheses; major differences between samples from Gredos and Alcolea-Córdoba indicated in square brackets preceded by G or A, respectively; Daimiel's sample does not include females. BL = 19.3 (13.2–26.6). Cephalothorax: Cl = 6.3 (4.8–8.2); Cw = 5.2 (4.0–6.6); C(l/w) = 1.21 (1.11–1.33); Ca = 4.0 (3.1–5.3); Ch/Th = 2.28 (1.98–2.71); Stl = 3.8 (2.9–4.9); Stw = 2.7 (2.1–3.6); St(l/w) = 1.38 (1.29–1.47); Ll = 0.5 (0.4–0.7); Lw = 1.3 (1.0–1.8); L(l/w) = 0.41 (0.31–0.49); Ml = 2.4 (1.9–3.0); Mw = 1.5 (1.2–2.0); M(l/w) = 1.61 (1.42–1.82), G [1.76 (1.73–1.82)]. Eye group: EL = 0.67 (0.52–0.77); AR = 1.27 (1.03–1.45); PR = 1.23 (0.98–1.47); AR/PR = 1.04 (0.99–1.08); AR/EL = 1.92 (1.69–2.06); AME = 0.29 (0.24–0.36); AMEi = 0.18 (0.12–0.21); AME−AME = 0.08 (0.05–0.12); ALE = 0.39 (0.28–0.47); PLE = 0.32 (0.24–0.41); ALE/PLE = 1.22 (0.98–1.52), G [(1.34 (1.19–1.48)]; PME = 0.20 (0.16–0.24); Cly = 0.29 (0.20–0.35); Cly/ALE = 0.76 (0.61–1.00); Cly/EL = 0.44 (0.36–0.52). Spinnerets (only fully extended spinnerets were measured): PLS = 1.74 (1.41–2.20) {PLSb = 1.07 (0.90–1.21); PLSm = 0.44 (0.29–0.69); PLSa = 0.23 (0.19–0.31)}. Appendages: palp = 10.3 (8.5–12.6) {Fe = 3.7 (3.1–4.5); Pa = 2.1 (1.7–2.6); Ti = 2.4 (2.0–3.0); Ta = 2.2 (1.7–2.6)}; leg I = 14.9 (12.4–18.4) {(Fe = 4.6 (3.6–5.8); Pa = 3.0 (2.4–3.9); Ti = 3.2 (2.7–4.0); Me = 2.5 (2.0–3.0); Ta = 1.7 (1.4–1.9)}; leg II = 13.6 (11.1–16.3) {(Fe = 4.1 (3.3–4.9); Pa = 2.7 (2.1–3.2); Ti = 2.7 (2.3–3.4); Me = 2.4 (2.0–2.9); Ta = 1.7 (1.4–1.9)}; leg

III = 13.0 (10.3–16.3) {(Fe = 3.7 (3.0–4.4); Pa = 2.4 (1.9–3.0); Ti = 2.2 (1.7–2.8); Me = 2.8 (2.2–3.6); Ta = 2.0 (1.5–2.5)}; leg IV = 18.7 (14.3–23.9) {(Fe = 4.7 (3.5–6.1); Pa = 3.2 (2.3–4.2); Ti = 4.7 (3.7–5.9); Me = 4.0 (3.1–5.0); Ta = 2.1 (1.7–2.8)}. Spermathecae: Se = 0.76 (0.52–1.15), G [0.87 (0.76–1.15)]; Si = 0.46 (0.32–0.77), G [0.55 (0.47– 0.77)]; Dw = 0.16 (0.10–0.20); Dh = 0.17 (0.10–0.25); Se/Dw = 4.96 (3.82–5.92), G [5.21 (4.71–5.92)]; Si/Dw = 3.02 (1.94–4.00), G [3.27 (2.76–3.95)]; Rh = 0.12 (0.10– 0.16); Rw = 0.19 (0.15–0.28); Dh/Rh = 1.42 (0.83–1.92), G [1.55 (1.39–1.81)]; Rw/Dw = 1.24 (0.98–1.71), G [1.10 (0.98–1.19)]; Sh = 0.36 (0.24–0.49); Sg = 0.29 (0.21–0.40); S(g/h) = 0.82 (0.74–0.87).

NATURAL HISTORY. Nest. *Iberesia castillana* digs galleries with compacted walls about 1.5 cm in diameter and 20 cm deep; the initial section of the tube is slightly inclined (sometimes horizontal depending on the obstacles in the ground; fig. 31A) and then deepens almost vertically. Burrows are closed by cork-type trapdoors with bevelled edges made of silk and soil (fig. 31B–C); the uppermost part of the tube is covered with a silk lining connected to the trapdoor by a silk hinge and forms a lateral widening below the hinge resembling that described in the nest of *I. valdemoriana* (Luis de la Iglesia, 2019a: fig. 28–30); one of the nests studied had a second opening with a typical trapdoor connected to the lateral widening (fig. 32A–B). Some prey remains (especially ants and beetles) were found at the bottom of the nest of specimens from Alcolea-Córdoba.

Habitat. Specimens from Gredos (Ávila; fig. 1) were found at altitudes between 400–800 m, on pasture margins and in *dehesas* (sparse holm oaks forests of *Quercus ilex*) and scrublands with few rockroses (*Cistus sp*) and brooms (*Cytisus scoparius*). They build their burrows next to bushes or in cleared areas, on loose granite sands. In Las Tablas de Daimiel (Ciudad Real; fig. 1), at about 600 m of altitude, they live in holm oak groves with few black hawthorn (*Ramnus lycioides*), asparagus (*Asparagus acutifolius*), thyme (*Thymus sp*), and other herbaceous species (Isla de Algeciras), or in halonitrophilic grasslands next to scarce shrub covers (*Suaeda vera*, *Limonium sp*) (Morano, 2017, pp. 23–24). Specimens from the Alcolea-Córdoba area (fig. 1) live at altitudes below 300 m, in *dehesas* (fig. 30) with holm oaks and wild olive trees with some stands of scrub of rockrose (*Cistus albidus*), thickets of kermes oak (*Quercus coccifera*) and mastic (*Pistacia lentiscus*) on a substrate formed by marls, calcarenites, limestones, dolomites and slates. Those from El Higuerón (Córdoba) were found in soil debris next to the railroad.

Phenology and behaviour. In Gredos wandering males fell into pitfall traps from October to mid-January with maximum captures in December (54.8%) and November (41.9%); however, in the period studied the traps produced no specimens after early rains in September and October. Data from Daimiel match these observations (Morano, 2017: graph 33), while in the Alcolea area the captures were more evenly distributed throughout the mating season (Oct = 10.0%, Nov = 30.0%, Dec = 25.0%, Jan = 35.0%). Females stay in their nests throughout the year; however, half of the females in the Gredos sample (4 out of 7) were collected from the same pitfall trap.

DISTRIBUTION (fig. 1). The specimens in our sample were recovered from various points in a vast area that extends over the territory of three Autonomous Communities in the centre and south of Spain mainland. In Castilla y León they were found in the province of Ávila, in the central sector (Arenas de San Pedro and Mombeltrán), and in the northeast limit of the southern slopes of Sierra de Gredos mountain range (El Tiemblo). In Castilla La Mancha, the species was found in the province of Ciudad Real (Las Tablas de Daimiel National Park, and Fuencaliente), and in Andalusia, in the province of Córdoba, municipalities of Córdoba, Alcolea and El Higuerón (see Table I). This suggests that the species may be present in all intermediate territories, and, probably, in neighbouring areas.

Discussion

Determination of *Iberesia castillana* and differences with *Iberesia machadoi*

The authors were able to examine photographic material of the holotype that is preserved in the MNHN, which allowed us to confirm that morphology and measurements of the males in our sample match those of the holotype. In addition, the males fully conform to the original description (Frade & Bacelar, 1931) but they do not quite fit well with the key to the species by Decae & Cardoso (2005, p. 5), whose statement «embolus tip smooth and only slightly bent», referred to two different characters, may be somewhat ambiguous. The first character, "embolus tip smooth", that is, absence of distal denticles in the embolus, can no longer be considered a determining diagnostic character, since the phenotype of the holotype falls within the range of variability of the sample (i.e., 0–3 tiny denticles). The second one, "embolus tip only slightly bent" may be inaccurate and does not seem to match the figures shown in their article, since the shape of bulbs of *I. machadoi* and *I. castillana* is similar both in ventral view (embolus tip sigmoid in the two species, see fig. 12 and 14 in Decae & Cardoso, 2005), and in lateral view (see fig. 26–27 in Zonstein, 2016). Size aside, there are few differences between their bulbs: in *I. machadoi* the embolus is proportionally shorter (Em/Lo = 1.1–1.3 in the specimens of *I. machadoi* in our material, n = 2; Em/Lo = 1.0 in Cardoso, 2000, p. 32), the S-shaped distal segment is wider, and the denticles are conspicuous (fig. 28B). In contrast, in *I. castillana*, both in the holotype (Em/Lo = 1.6; as measured from Decae & Cardoso, 2005: fig. 14) and in our sample (average Em/Lo = 1.5, n = 60), the embolus is longer, the S-shaped segment is shorter, and the denticles, if any, are hardly apparent (compare fig. 4B, 33C with fig. 34C & fig. 2E, 4A, 19A–F).

In addition, there are other morphological differences that allow to easily distinguish males from both species. *Body size*: BL = 16.7–18.2 in *I. machadoi* (Decae & Cardoso, 2005, p. 8; Decae *et al.*, 2007, p. 9) (fig. 33A), BL = 13.0 in the holotype of *I. castillana* (fig. 34A), BL = 9.6–15.8, in our material (fig. 10, 13). *Palpal tibia*: its shape is markedly different in both species (see the key to species above; compare fig. 3B, 33D with fig. 3A, 34D & fig. 2C, 16C). *Sternal sigilla:* the three pairs well visible in *I. machadoi*, where the posterior sigilla are separated from the sternal margin by a distance about twice their long axis (fig. 5B) whereas in *I. castillana* the anterior and intermediate sigilla are barely perceptible and the posterior are closer to the sternal margin (fig. 5A). *Clypeus and Cly/ALE, Cly/EL ratios*: higher in *I. machadoi* (Cly = 0.42, Cly/ALE = 1.00, Cly/EL = 0.64; fig. 33B) than in the holotype of *I. castillana* (Cly = 0.26, Cly/ALE = 0.72, Cly/EL = 0.42; fig. 34B) and in our sample

(average, Cly = 0.22, Cly/ALE = 0.72, Cly/EL = 0.43; fig. 12). We have not observed that the measurements of each of these two characters overlap in the specimens of the two species present in our material, nor have we found it in the literature (Frade & Bacelar, 1931; Cardoso, 2000; Zonstein, 2016; Luis de la Iglesia, 2019a). *Macro-spigots:* the distal segment of the PLS of *I. castillana* has always a solitary central macro-spigot (fig. 15A–B), while in *I. machadoi* there are 2–3 larger macro-spigots. *Epiandrous spigots:* the density of spigots of epiandrous apparatus is noticeable higher in *I. castillana* (average, 106.7 spigots/mm^2) than in *I. machadoi* (average, 54.5 spigots/mm^2). *Eye formation*: the rectangle formed by the eyes seems lower and wider in the specimens of *I. machadoi* we have examined (AR/EL = 2.2; also in Cardoso, 2000, p. 32; *cf.* fig. 33B, 12, 34B) but there is some overlapping in these measurements when larger samples are studied (see morphometric variation above, and in Decae & Cardoso, 2005, p. 8). Finally, the angle formed by the axes of the ALE and PLE is appreciably lower in *I. machadoi* (85º, fig. 33B) than in *I. castillana* (average 105º, dorsal view, fig. 12, 34B).

The most obvious difference between the two species lies in the female sexual organs; the mere examination of the spermathecae of both species leaves no room for doubt (*cf.* fig. 8A; 2D, 8F, 29A–F). Moreover, other characters also show significant differences. *Body length:* large-sized in *I. machadoi* (BL = 19.9–29.1, n = 10, Decae & Cardoso, 2005), medium-sized in *I. castillana* (13.2–26.6, n = 23). *Clypeus:* almost twice the length of ALE and almost equal to EL in *I. machadoi* (Cly/ALE = 1.86, Cly/EL = 0.99; fig. 7A) but clearly smaller in *I. castillana* (Cly/ALE = 0.76, Cly/EL = 0.44; fig. 7B). *Sigilla:* same differences as in the male *(cf.* fig. 6A, 6B). *Maxillary cuspules:* thin and pointed in *I. machadoi*, but thick and blunt in *I. castillana*. *Eye formation:* lower and wider in *I. machadoi* (fig. 7A; AR/EL = 2.2) than in *I. castillana* (fig. 7B, AR/EL = 1.7–2.1); all eyes are proportionally smaller in *I. machadoi*; the distance between both AME is notably greater in *I. machadoi* than in *I. castillana*; and finally, ALE & PLE are similarly sized in *I. machadoi*, but different in *I. castillana* (ALE/PLE = 1.22) (fig. 7A–B). Again, as in males, there is some overlap in the eye formation measurements of the two species (compare morphometric data above with those of Decae & Cardoso, 2005, p. 8).

Population differences

The main goal of this work was to rediscover and re-describe the species *Iberesia castillana*, which has been so elusive to researchers since it was first described in 1931, so we focused our sampling in the province of Ávila. When we examined our material, we realized that the main morphological characters of the males from Gredos were identical to those of some specimens from Alcolea and Córdoba studied in the End-Of-Degree Project of one of the authors (Pertegal, 2019). In addition, the similarity in the bulb of *I. machadoi* and *I. castillana* led us to assume that other records of *I. machadoi* in the Iberian Peninsula could have been identified in error (an idea already suggested, Decae & Cardoso, 2005, p. 10), so we decided to re-examine our material and tried to review the records of *I. machadoi* reported in Spain requesting the collaboration of the authors (Sánchez, 2012; Morano, 2017; Alameda-Lozano, 2018; González Moliné, 2018; Barrientos *et al.*, 2019) in order to confirm this hypothesis. This allowed us to confirm, so far, the presence of *I. machadoi* in Plasencia and Villarreal de San Carlos (Cáceres, see Table I), in Puebla de Sancho Pérez (Badajoz, see Table I), and in Burguillos del Cerro (Badajoz; Alameda-Lozano, 2018), and to notice the occurrence of *I. castillana* instead of *I. machadoi* in PNTD, Ciudad Real (Morano, 2017). Finally, the examination of a male from Monte Valcorchero (Plasencia, Cáceres) provisionally identified as *Iberesia* prope *machadoi* (Barrientos *et al.* 2019), revealed that it was a male of *Nemesia athiasi* Franganillo, 1920.

Within our sample of *Iberesia castillana*, along with main shared characters, we also found some population differences in the male colour patterns, the female lateral eyes, and the female sexual organs. *Male colour patterns:* males in the Gredos sample are usually darker, ranging from the bicolour pattern typical of the genus (i.e., dark brown caput and chelicerae, orange thorax, fig. 9B, 10A) to the dark pattern (dark brown cephalothorax and chelicerae, fig. 10B; 61% of the males in the Gredos sample), while colour patterns in the Daimiel and Alcolea males vary from the bicolour pattern to lighter orange patterns (fig. 10C), with the caput and chelicerae only slightly darker (this may be due in part to fading of the specimens in the preservation medium). *Female lateral eyes:* ALE/PLE is higher in Gredos females (average, 1.34, fig. 24A) than in Alcolea-Córdoba females (average, 1.17, fig. 24B). *Female sexual organs*: the separation between the spermathecae is smaller in Alcolea-Córdoba females than in Gredos females (compare fig. 29A–C with fig. 29D–F), so there are also differences in the Se/Dw and Si/Dw ratios (5.21 *vs.* 4.82, and 3.27 *vs.* 2.89, respectively).

Intrapopulation variation

The population diversity described above is added to a wide intraspecific variation found within each population. This observation is in line with growing evidence of some degree of variation in some characters including sexual organs (embolic denticles: Luis de la Iglesia, 2019a, present work; spermathecae: Blasco, 1986b, present work) as well as other characters with diagnostic value (see Decae, 2005, pp. 147–149; Decae & Cardoso, 2005, p. 4; Decae, Cardoso & Selden, 2007, pp. 2–3) as colour patterns, POP patterns, crest setae, fringe setae, patellar & leg IV formulae, cheliceral furrow teeth, cheliceral fang keel, fovea central groove (Decae, 2005, Decae & Cardoso, 2005, Decae, Cardoso & Selden, 2007; Luis de la Iglesia, 2019a,b). For example, differences have been observed in the fang serration within individuals of the same sex of some Balearic (*Nemesia bristowei* Decae, 2005, *N. ibiza* Decae, 2005) and Portuguese *Nemesia* species (*N. athiasi*; *N. fagei* Frade & Bacelar, 1931; and *N. bacelarae* Decae, Cardoso & Selden, 2007; Decae *et al.*, 2007; Luis de la Iglesia, 2019b), and something similar is observed with the central groove of the fovea in *N. athiasi* (Decae *et al.* 2007) and *I. castillana* (see above).

Conversely, two characters that vary frequently in related species remain highly conserved in our sample, namely, the number of cheliceral teeth and the number of macrospigots in the distal segment of the PMS. Thus, in other known species of the genus, the number of cheliceral teeth ranges from 5 to 7 (Koch, 1882; Cardoso, 2000; Decae, 2005; Decae & Cardoso, 2005; Calvo, 2020), and even reaches 8–9 (Luis de la Iglesia, 2009a), usually due to the addition of 1–2 small teeth between those occupying positions 1 and 2. However, in our sample the number of teeth is 6 in 91.2% of

males and 92.3% of females, and extra teeth often occupy "ectopic" positions, such as far behind the sixth tooth (fig. 14A), or between the fifth and sixth teeth. Similarly, the number of macro-spigots in the distal segment of the PMS generally ranges from 1 to 3 in males of related species (personal observation), but there is always one solitary macrospigot in all males of *I. castillana* examined so far.

Given the similarities and differences that we have just described, we have concluded that these three populations belong to the same species and that this species cannot be different from *Iberesia castillana*. However, the molecular genetic characterization of specimens of these three populations (something beyond the objective and methodology of our work), would probably clear any doubt about the definitive affiliation of these populations, a task that remains pending for future research.

Acknowledgment

We wish to thank the effort and dedication of our relatives M. Ángeles Báez, Sergio Luis and Mariano Pagán in the installation, handling, and collection of specimens of the pitfall traps installed in the province of Ávila. We are especially indebted to Eduardo Morano, who unconditionally offered his help and generously made some of the material from the PNTD study of spiders available to us. Our gratitude is also due to José Antonio Barrientos, Alberto Narro, Javier Alameda, Íñigo Sáchez, Ginés Rodríguez, Fernando Goytre, and Rafael Tamajón, who have handed us specimens of their collections or have provided us with useful information. We also thank the "Delegación Territorial de Agricultura, Ganadería, Pesca y Desarrollo Sostenible" of Córdoba for the authorization to collect specimens for the study. The authors really appreciate everything Mrs Elise-Anne Leguin and the MNHN have done to make available to us the photographs that allowed us to compare our material with the holotype of *Iberesia castillana*. Finally, we thank Prof. Eduardo Burrieza who has helped us improve the English version of the original manuscript.

References

ALAMEDA-LOZANO, J. 2018. Contribución al conocimiento de las arañas (Araneae) de la provincia de Badajoz (Extremadura, España). *Revista Ibérica de Aracnología*, **32**: 21–30.

BARRIENTOS, J. A. & M. A. FERRÁNDEZ 1981. La colección de Araneidos del Departamento de Zoología de la Universidad de Salamanca, III: arañas migalomorfas, haploginas, y cribeladas. *Boletín de la Asociación Española de Entomología*, **5**: 75–86.

BARRIENTOS, J. A. & C. GÓMEZ 2014. Nota breve sobre algunas arañas (Arachnida, Araneae) de Olmedo (Valladolid, España). *Revista Ibérica de Aracnología*, **24**: 104–106.*

BARRIENTOS, J. A., R. GARCÍA-SARRIÓN, I. URIBARRI, C. E. PRIETO & J. ALAMEDA LOZANO 2019. Algunas arañas (Araneae) del Monte Valcorchero (Plasencia, Cáceres, España). *Revista Ibérica de Aracnología*, **34**: 87–96.*

BLASCO, A. 1986a. El género *Nemesia* Audouin, 1925. (Arachnida: Ctenizidae) en Cataluña. *Publicaciones del Departamento de Zoología; Universidad de Barcelona* **12**: 41–49.

BLASCO-FELIU, A. 1986b. Les spermathèques des *Nemesia* (Araneae, Ctenizidae); valeur taxonomique de ce caractère. *Bulletin du Muséum National d'Histoire Naturelle de Paris*, **8**(4): 343–350.

CALVO G., M. 2020. *Iberesia arturica* sp. n.; descripción de una nueva especie de *Iberesia* Decae & Cardoso, 2005 (Araneae, Mygalomorphae, Nemesiidae) de la Península Ibérica. *Revista Ibérica de Aracnología*, **36**: 13–23.*

CARDOSO, P. 2000. Description of the supposed male *Nemesia hispanica* L. Koch in Ausserer, 1871 (Araneae: Nemesiidae). *Ekológia (Bratislava)*, **19**(Suppl. 3): 31–36.

DECAE, A. E. 1995. Two new trapdoor spider species in the genus *Nemesia* Audouin, 1827 and the first report of this genus from Greece (Araneae, Mygalomorphae, Nemesiidae). *Deinsea*, **2**: 1–8.

DECAE, A. E. 2005. Trapdoor spiders of the genus *Nemesia* Audouin, 1826 on Majorca and Ibiza: taxonomy, distribution and behaviour (Araneae, Mygalomorphae, Nemesiidae). *Bulletin of the British Arachnological Society*, **13**: 145−168.

DECAE, A. E. 2012. Geography-related sub-generic diversity within the Mediterranean trapdoor spider genus *Nemesia* (Araneae, Mygalomorphae, Nemesiidae). *Arachnologische Mitteilungen*, **43**: 24−28.

DECAE, A. & S. HUBER 2017. Description of a new *Nemesia* species from Sardinia that constructs a remarkable star-shaped trapdoor (Araneae: Mygalomorphae: Nemesiidae). *Arachnology*, **17**(4): 188−194.

DECAE, A. E. & P. CARDOSO 2005: *Iberesia*, a new genus of trapdoor spiders (Araneae, Nemesiidae) from Portugal and Spain. *Revista Ibérica de Aracnología*, **12**: 3–11.*

DECAE, A., P. CARDOSO & P. SELDEN 2007. Taxonomic review of the Portuguese Nemesiidae (Araneae, Mygalomorphae). *Revista Ibérica de Aracnología*, **14**: 1−18.*

FAGE, L. & A. DE B. MACHADO 1951. Quelques particularités remarquables de l'anatomie des ochyrocératides (Araneae). *Archives de Zoologie Expérimentale et Générale*, **87**: 95–103.

FERRETTI, N., G. POMPOZZI, S. COPPERI, A. WEHITT, E. GALÍNDEZ, A. GONZÁLEZ & F. PÉREZ-MILES 2017. A comparative morphological study of the epiandrous apparatus in mygalomorph spiders (Araneae, Mygalomorphae). *Micron*, **93**: 9–19,

FRADE, M. A. & A. BACELAR 1931. Remarques sur trois araignées théraphoses de Sicile et du nord d'Afrique. *Bulletin du Muséum National d'Histoire Naturelle de Paris*, **3**(2): 125 –130.

FRANGANILLO B., P. 1920. Contribution à l'étude des arachnides du Portugal. *Boletim da Sociedade Portuguesa de Ciencias Naturais*, **8**: 138–144.

GONZÁLEZ-MOLINÉ, A. L. 2018. Catalogue of the spiders (Araneae) of Huelva province, Iberian Peninsula. *Revista Ibérica de Aracnología*, **32**: 37–50.*

KOCH, L. 1882. Zoologische Ergebnisse von Excursionen auf den Balearen. II: Arachniden und Myriapoden. *Verhandlungen der Kaiserlich-Königlichen Zoologisch-Botanischen Gesellschaft in Wien*, **31**: 625−678.

LE PERU, B. 2011. The Spiders of Europe, a synthesis of data (volume 1) Atypidae to Theridiidae. *Mémoires de la Société Linnéenne de Lyon*, **2**: 1−522.

LOPEZ, A. & M. EMERIT 1988. New data on the epigastric apparatus of male spiders. *Bulletin of the British Arachnological Society*, **7**(7): 220–224.

LUCAS, H. 1846. Histoire naturelle des animaux articulés. In: *Exploration scientifique de l'Algérie pendant les années 1840, 1841, 1842 publiée par ordre du Gouvernement et avec le concours d'une commission académique. Première Partie. Crustacés, Arachnides, Myriapodes et Hexapodes. Paris, Sciences physiques, Zoologie* **1**: 89−90.

LUIS DE LA IGLESIA, J. A. 2019a. A new Iberian trapdoor spider, *Iberesia valdemoriana* n. sp., and the first records of *I. brauni* and *I. barbara* in the Iberian Peninsula (Araneae: Nemesiidae). *Arachnology*, **18**(2): 156–171.

LUIS DE LA IGLESIA, J. A. 2019b. Primera cita en España de *Nemesia bacelarae* Decae, Cardoso & Selden, 2007 (Araneae: Nemesiidae). *Revista Ibérica de Aracnología*, **36**: 91–96.*

MACHADO, A. DE B. 1951. Ochyroceratidae (Araneae) de l'Angola. *Publicações culturais da Companhia de Diamantes de Angola*, **8**: 9–87.

MARPLES, B.J. 1967. The spinnerets and epiandrous glands of spiders. *Zoological Journal of the Linnean Society*, **46**(310): 209–223.

MICHALIK, P. & G. UHL 2005. The male genital system of the cellar spider *Pholcus phalangioides* (Fuesslin, 1775) (Pholcidae,

Araneae): development of spermatozoa and seminal secretion. *Frontiers in Zoology*, **2**(1): 1–12.

MOLERO-BALTANÁS, R., M. GAJÚ-RICART & C. BACH DE ROCA 2000. On the taxonomic use of the distribution pattern of the antenna asteriform sensilla in *Neoasterolepisma* and *Tricholepisma* (Insecta, Zygentoma, Lepismatidae). *Pedobiologia*, **44**: 248–256.

MORA, E. C. 2015. Evolutionary history and drivers of diversification of the Mediterranean Nemesiidae spiders (Araneae, Mygalomorphae). Ph.D. Thesis, University of Barcelona [unpublished].

MORANO, E. 2017. *Arañas del Parque nacional de las Tablas de Daimiel.* Editorial Organismo Autónomo Parques Nacionales. 200 pp

PÉREZ MILES, F. & C. PERAFÁN 2017. Behavior and Biology of Mygalomorphae. Pp. 29–54, in Viera C. & M. O. Gonzaga (eds.) *Behavior and Ecology of Spiders: Contributions from the Neotropical Region*. Springer, Cham, XVII, 437 pp.

PERTEGAL P., C. 2019. Estudio faunístico y biológico comparado de los Migalomorpha de dos sectores biogeográficos de Andalucía. End-Of-Degree Project, University of Córdoba [unpublished].

SÁNCHEZ, I. 2012. Adiciones y correcciones al catálogo de las arañas (Araneae) de la provincia de Cádiz. *Revista de la Sociedad Gaditana de Historia Natural*, **6**: 31–46.

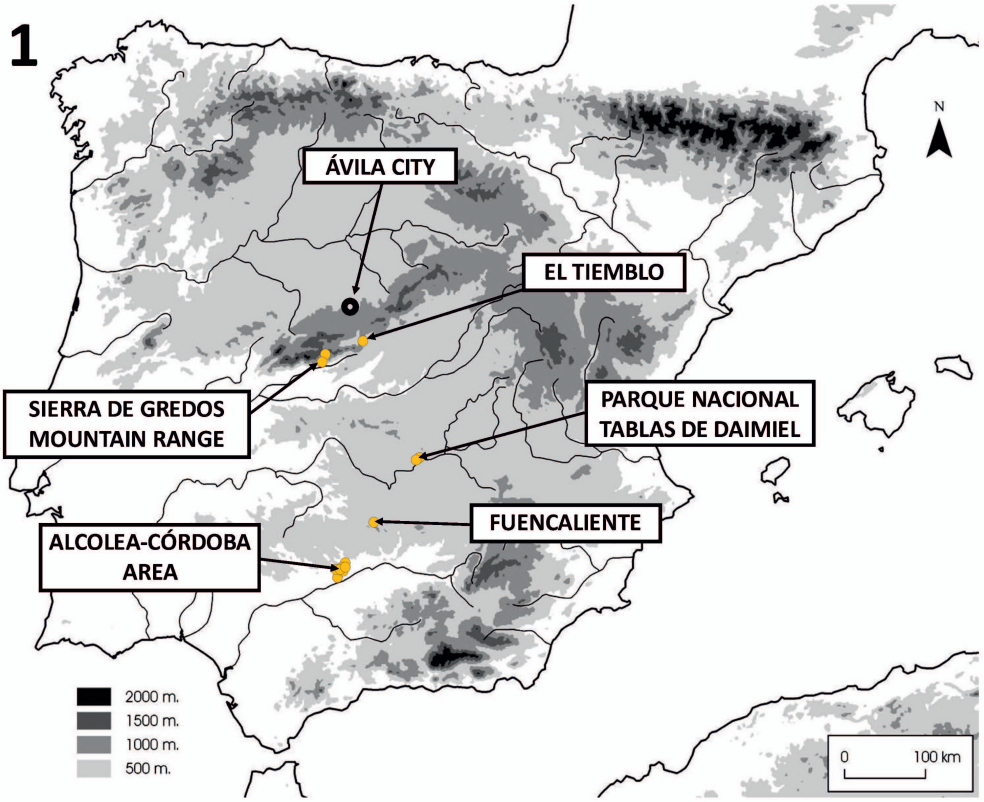
ZONSTEIN, S. 2009. A review of the mygalomorph spiders of the *Raveniola caudata* species-group (Araneae, Nemesiidae) *Zootaxa*, **2217**: 37−42.

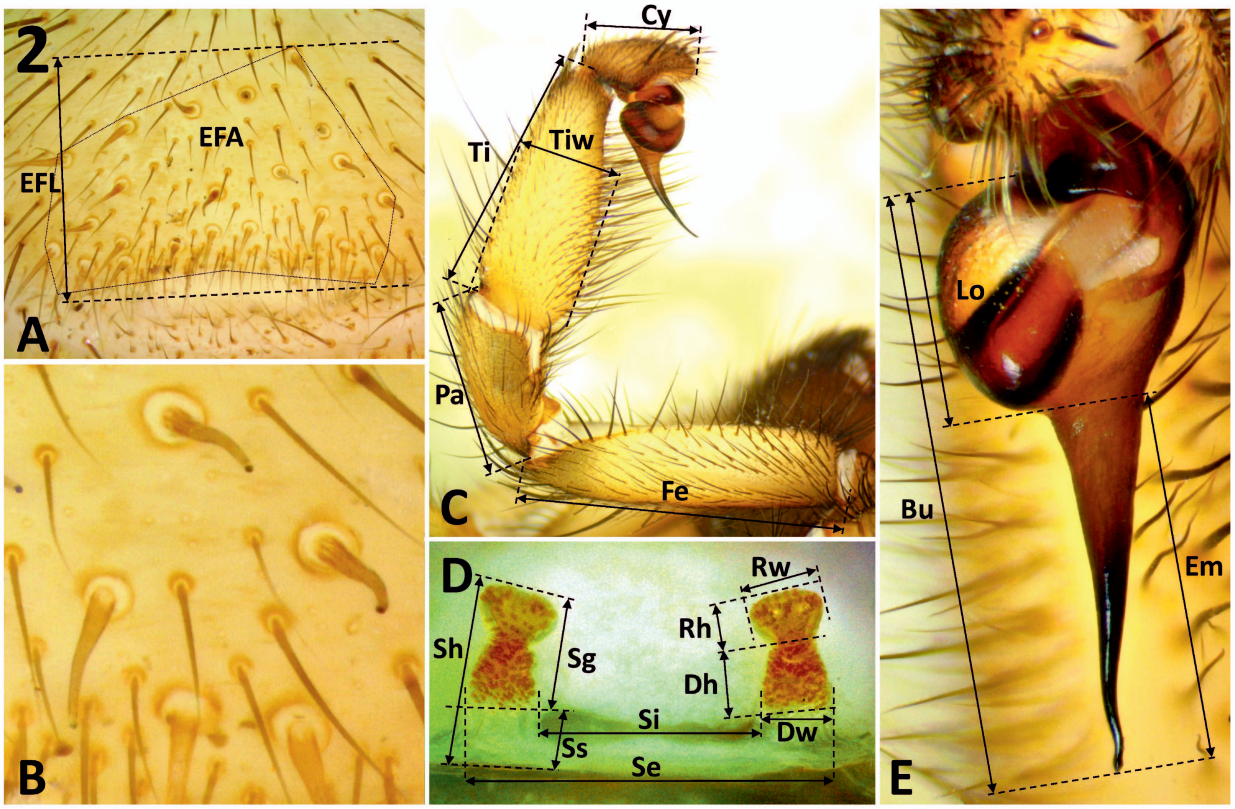
ZONSTEIN, S. L. 2016. A redescription and synonymy of North African mygalomorph *Iberesia barbara* (Lucas, 1846), comb. n. (Aranei: Nemesiidae). *Arthropoda Selecta*, **25**: 385−393.

* References available at www.sea-enomologia.org

► **Fig. 1.** Map indicating the location in mainland Spain of the *Iberesia castillana* populations used in this study. // **Fig. 1.** Mapa que señala la ubicación en España peninsular de las poblaciones de *Iberesia castillana* usadas en este estudio.

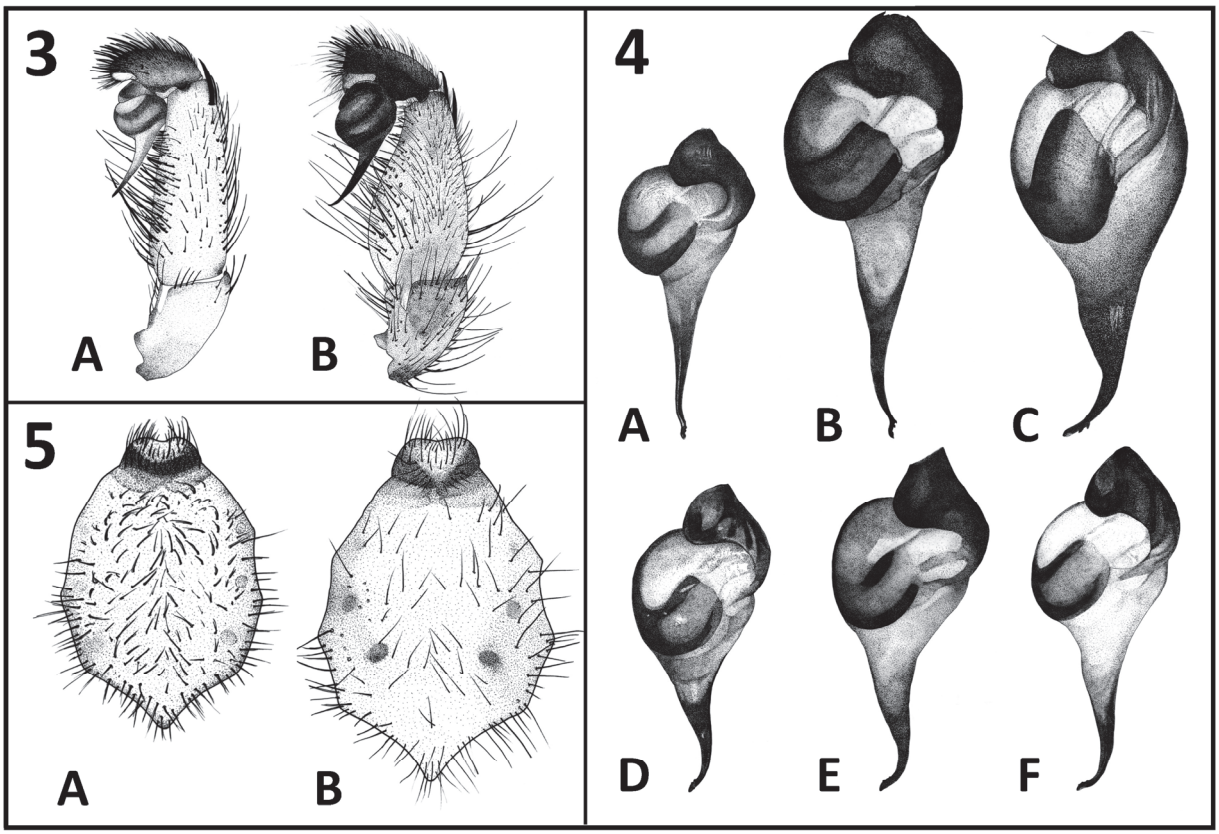
► **Fig. 2.** Some new measurements and ratios. A–B. Male epiandrous apparatus (#JAL–1247–AVT40). A. Epiandrous spigot field area, EFA, and epiandrous spigot field length, EFL. B. Epiandrous spigots. C. Male palp: Ti/Tiw, new ratio that partly describes the shape of the palpal tibia (#JAL–1247–AVT40). D. Spermathecae ratios: Dh/Rh, Rw/Dw, Se/Dw, Si/Dw, S(g/h), S(g/s) (#MNHN AR16178). E. Bulb ratios: Bu/Em, Em/Lo (#JAL–1247–AVT40). See abbreviations in the text. // **Fig. 2.** Algunas nuevas medidas y ratios. A–B. Aparato epiándrico del macho (#JAL–1247–AVT40). A. Campo de fúsulas epiándricas; área y longitud del campo, EFA y EFL, respectivamente. B. Fúsulas epidándricas. C. Palpo del macho (#JAL–1247–AVT40); la nueva ratio Ti/Tiw describe en parte la forma de la tibia del palpo. D. Ratios de las espermatecas: Dh/Rh, Rw/Dw, Se/Dw, Si/Dw, S(g/h), S(g/s) ((#MNHN AR16178). E. Ratios del bulbo: Bu/Em, Em/Lo (#JAL–1247–AVT40). Abreviaturas en el texto.

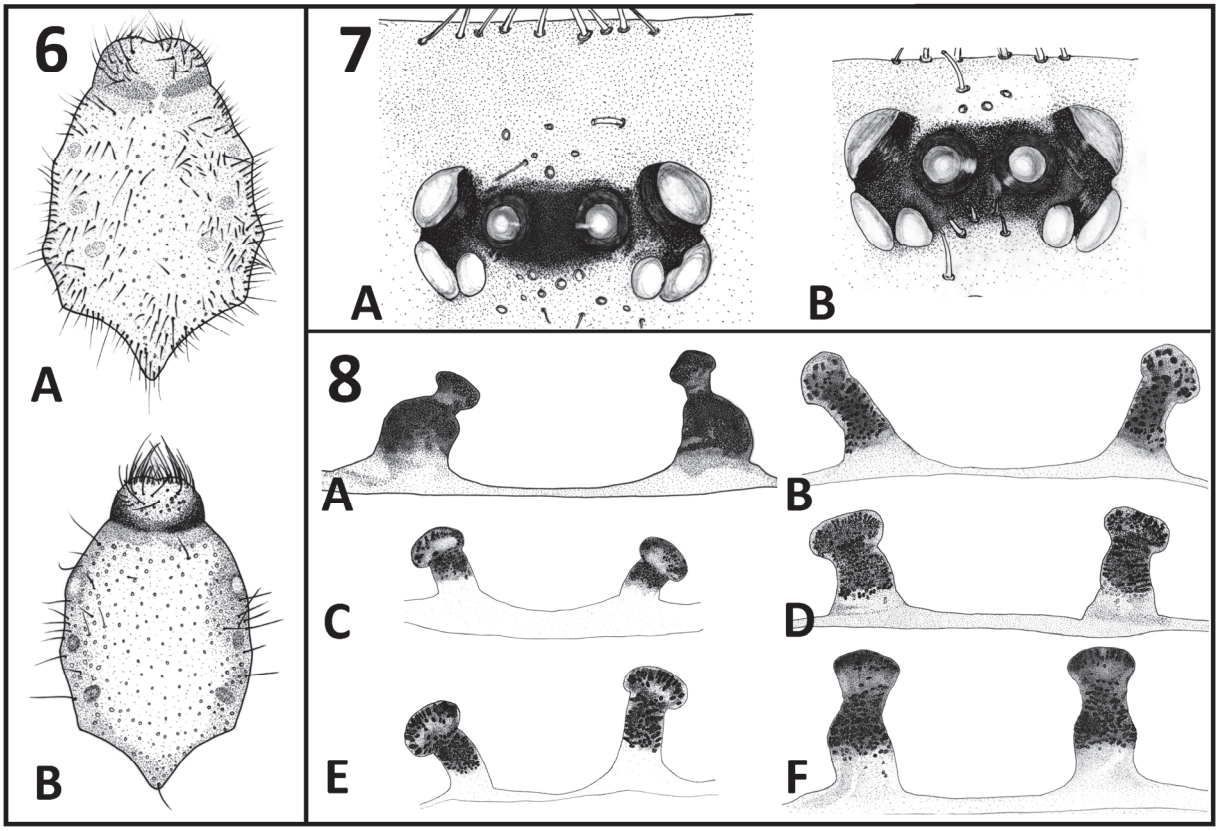

1
ÁVILA CITY
EL TIEMBLO
SIERRA DE GREDOS
MOUNTAIN RANGE
PARQUE NACIONAL
TABLAS DE DAIMIEL
FUENCALIENTE
ALCOLEA-CÓRDOBA
AREA
2000 m.
1500 m.
1000 m.
500 m.
N
0
100 km


2
EFA
EFL
A
B
Cy
Ti
Tiw
Pa
Fe
C
D
Rw
Sh
Sg
Rh
Dh
Si
Dw
Ss
Se
Lo
Bu
Em
E

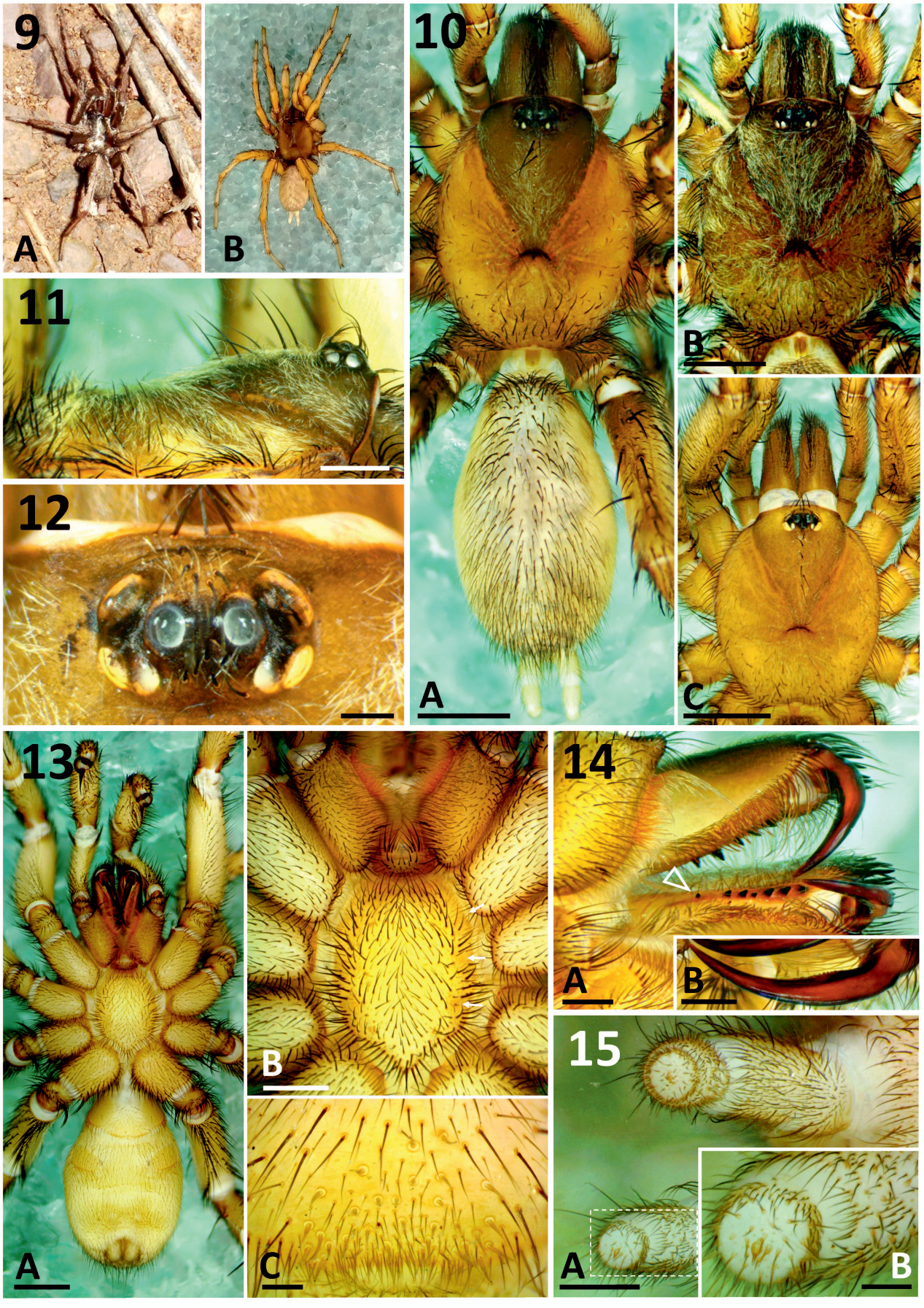
► **Fig. 3–5.** Illustrations of the key to the species of genus *Iberesia*, males. 3. Shape of palpal tibia. A. Narrow tibia (*I. castillana*, drawn from a photograph of the holotype #MNHN AR4341). B. Tibia thickened at its base (*I. machadoi*, #CCPP–0030). 4. Shape of bulb. A. Short proximal lobe, sigmoid embolus, tiny or missing embolic teeth (*I. castillana*, #MNCN 20.02/19859). B. Large proximal lobe, sigmoid embolus, prominent teeth (*I. machadoi*, #M20170113–1). C. Large proximal lobe, curved embolus, prominent teeth (*I. arturica*, #JAL–1359). D. Short, curved embolus, small teeth (*I. brauni*, #M20171105–1). E. Curved embolus, tiny teeth (*I. barbara*, drawn from a photograph of male #MNHN 6163/AR4486, courtesy of Dr. S. Zonstein). F. Long, curved embolus, narrow embolus base, small teeth (*I. valdemoriana*, drawn from the holotype #MNCN 20.02/19345). 5. Position of sternal sigilla. A. Sigilla near the sternum margin (*I. castillana*, #CCPP–0029–3). B. Sigilla separated from the sternum margin (*I. machadoi*, #CCPP–0030). Line drawings not to scale. // **Fig. 3–5.** Ilustraciones de la clave para la determinación de especies del género *Iberesia*, machos. 3. Forma de la tibia del palpo. A. Tibia estrecha (*I. castillana*, dibujada de una fotografía del holotipo #MNHN AR4341). B. Tibia engrosada en su base (*I. machadoi*, #CCPP–0030). 4. Forma del bulbo. A. Lóbulo proximal corto, émbolo sigmoideo, dientes del émbolo diminutos o ausentes (*I. castillana*, #MNCN 20.02/19859). B. Lóbulo grande, émbolo sigmoideo, dientes prominentes (*I. machadoi*, #M20170113–1). C. Lóbulo grande, émbolo curvo, dientes prominentes (*I. arturica*, #JAL–1359). D. Émbolo corto y curvo, dientes pequeños (*I. brauni*, #M20171105–1). E. Émbolo curvo, dientes diminutos (*I. barbara*, dibujado de una fotografía del macho #MNHN 6163/AR 4486, cortesía del Dr. S. Zonstein). F. Émbolo largo y curvo, base del émbolo estrecha; dientes pequeños (*I. valdemoriana*, dibujado de una fotografía del holotipo #MNCN 20.02/19345). Los dibujos no están a la misma escala. 5. Posición de las sigilas esternales. A. Próximas al margen del esternón (*I. castillana*, #CCPP–0029–3). B. Alejadas del margen del esternón (*I. machadoi*, #CCPP–0030).

► **Fig. 6–8.** Illustrations of the key to the species of genus *Iberesia*, females. 6. Position of sternal sigilla. A. Sigilla separated from the margin (*I. machadoi*, #M20171013–2). B. Sigilla near the margin (*I. castillana*, #CCPP–0084). 7. Clypeus and eye group. A. Clypeus hight, eye group short and wide (*I. machadoi*, #M20171013–2). B. Clypeus low, eye group long and narrow (*I. castillana*, #JAL–1259–AVT40). 8. Spermathecae. A. Tripartite spermathecae (*I. machadoi*, #M20171012-1). B. Bipartite spermathecae, ducts diverging, basal part narrow (*I. arturica*, #JAL–1271). C. Bipartite spermathecae, ducts short (*I. brauni*, #JAL–735). D. Bipartite spermathecae, duct width as the receptacles or slightly wider (*I. barbara*, drawn from a photograph of the female #MNHN 6143/AR4481, courtesy of Dr. S. Zonstein). E. Bipartite spermathecae, long, tube-shaped ducts (*I. valdemoriana*, #JAL–731). F. Bipartite spermathecae, barrel-shaped ducts (*I. castillana*, #JAL–1293). // **Fig. 6–8.** Ilustraciones de la clave para la determinación de especies del género *Iberesia*, hembras. 6. Posición de las sigilas esternales. A. Sigilas separadas del margen del esternón (*I. machadoi*, #M20171013–2). B. Sigilas próximas al margen (*I. castillana*, #CCPP–0084). 7. Clípeo y formación ocular. A. Clípeo largo, grupo ocular corto y ancho (*I. machadoi*, #M20171013–2). B. Clípeo corto, grupo ocular largo y estrecho (*I. castillana*, #JAL–1259–AVT40). 8. Espermatecas. A. Espermatecas tripartitas (*I. machadoi*, #M20171012–1). B. Espermatecas bipartitas, conductos divergentes (*I. arturica*, #JAL–1271). C. Espermatecas bipartitas, conductos cortos (*I. brauni*, #JAL–735). D. Espermatecas bipartitas, anchura de los conductos igual o algo mayor que los receptáculos (*I. barbara*, dibujada de una fotografía de la hembra #MNHN 6143/AR4481, cortesía del Dr. S. Zonstein). E. Espermatecas bipartitas, conductos tubulares largos (*I. valdemoriana*, #JAL–731). F. Espermatecas bipartitas, conductos en forma de tonel (*I. castillana*, #JAL–1293).

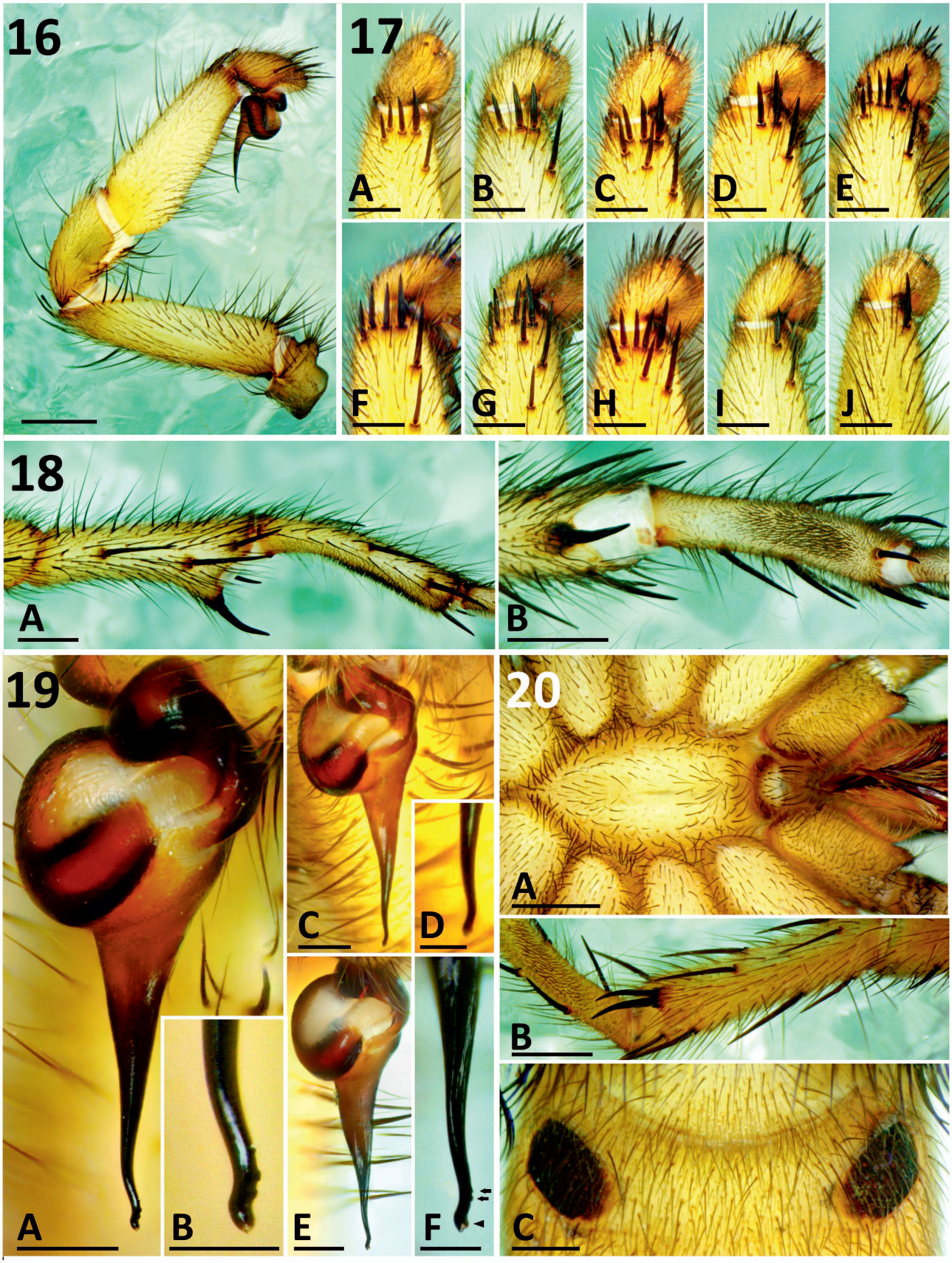

3
A
B
4
A
B
C
D
E
F
5
A
B


6
A
B
7
A
B
8
A
B
C
D
E
F

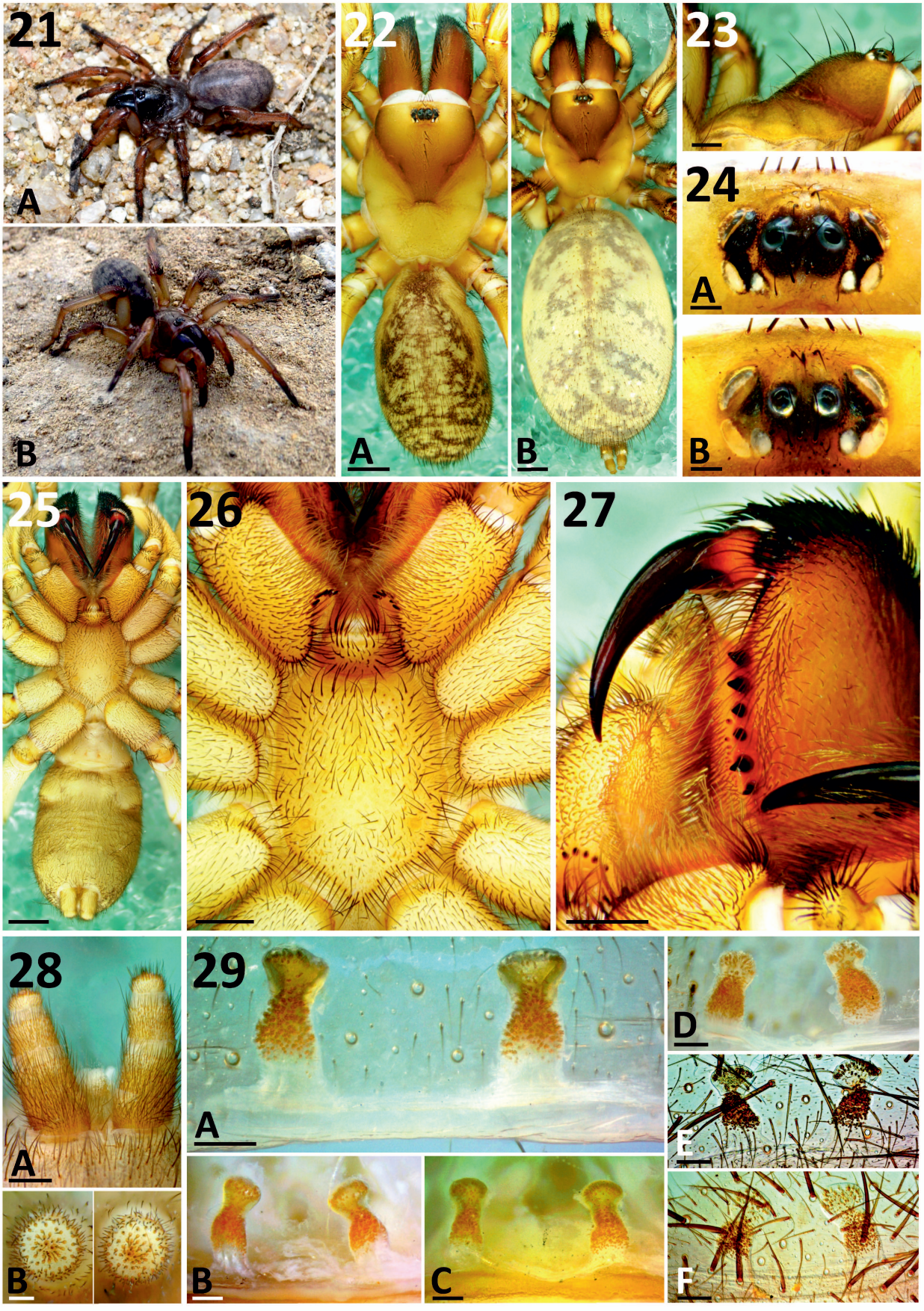
► **Fig. 9–15.** Male of *Iberesia castillana*. 9. Habitus and coloration. A. Living specimen (#MIG–056a). B. Preserved specimen (#JAL–1121–AVT40). 10. Different colour patterns. A. Bicolour pattern (#MNCN 20.02/19859). B. Dark pattern (#MNCN 20.02/19860). C. Light pattern (#MIG–18b). 11. Carapace, lateral view (#JAL–1127–AVT40). 12. Eye group (#JAL–1121–AVT40). 13. Ventral view. A. Habitus (#JAL–1126–AVT40). B. Sternum, labium, and maxillae; arrows point to sigilla, barely visible as slightly darker spots (#JAL–1134–AVT41). C. Epiandrous apparatus (#JAL–1121–AVT40). 14. Maxillae and chelicerae, ventral view (#JAL–1134–AVT41). A. Maxillae: note the blunt anterior process (top) and the single row of five setiform cuspules (bottom). Chelicerae: the triangle points to a small extra tooth in an unusual "ectopic" position. B. Cheliceral fang; note the serration of the prolateral keel. 15. Spinnerets (#JAL–1121–AVT40). A. Posterior lateral spinnerets, ventral view. B. Detail of rectangle shown in A; apical segment of left PLS showing few spigots surrounding a single central macro-spigot. Scale bars: 2.00 mm (10A–C, 13A); 1.00 mm (11, 13B); 0.50 mm (14A–B, 8A); 0.25 mm (12); 0.15 (13C, 15B). // **Fig. 9–15.** Macho de *Iberesia castillana*. 9. Habitus y coloración. A. Ejemplar vivo (#MIG–056a). B. Ejemplar conservado (#JAL–1121–AVT40). 10. Diferentes facies pigmentarias. A. Facies bicolor (#MNCN 20.02/19859). B. Facies oscura (#MNCN 20.02/19860). C. Facies clara (#MIG–18b). 11. Caparazón, vista lateral (#JAL–1127–AVT40). 12. Formación ocular (#JAL–1121–AVT40). 13. Vista ventral. A. Habitus (#JAL–1126–AVT40). B. Esternón, labio y maxilas; las flechas señalan las sigilas, apenas visibles como manchas algo más oscuras (#JAL–1134–AVT41). C. Aparato epiándrico (#JAL–1121–AVT40). 14. Maxilas y quelíceros, vista ventral (#JAL–1134–AVT41). A. Maxilas: nótese el proceso anterior romo (arriba) y la fila única de cinco cúspulas setiformes (abajo). Quelíceros: el triángulo apunta hacia un pequeño diente extra que ocupa una posición “ectópica” inusual. B. Colmillo del quelícero; nótese el filo prolateral serrado. 15. Hileras (#JAL–1121–AVT40). A. Hileras laterales posteriores, vista ventral. B. Detalle del rectángulo mostrado en A; segmento apical de la hilera posterior lateral izquierda en el que se observan algunas fúsulas que rodean una única macrofúsula central. Barras de escala: 2,00 mm (10A–C, 13A); 1,00 mm (11, 13B); 0,50 mm (14A–B, 15A); 0,25 mm (12); 0,15 (13C, 15B).


9
A
B
10
A
B
C
11
12
13
A
B
C
14
A
B
15
A
B

► **Fig. 16–20.** Male of *Iberesia castillana* (continued). 16. Right palp, retrolateral view (#MNCN 20.02/19859). 17. Different spine alignments in the dorsoapical rake of the palpal tibia, ordered from more frequent (A–C) to less frequent (G–J); slightly prodorsal view (not all spine alignments found are shown). A. 3+1+1 (#JAL–1120–AVT40). B. 3+0+1 (#JAL–1121–AVT40). C. 3+2+1 (#JAL–1120–AVT40). D. 2+0+1 (#CCPP–0029–1). E. 4+1+1 (#JAL–1258–AVT40). F. 3+1+1+1 (#CCPP–0029–2). G. 3+2+1+1 (#MIG–056f). H. 4+2+1 (#MIG–056c). I. 1+0+1 (#JAL–1122–AVT40). J. 1+0+0 (#MIG–056f). 18. Clasper, left leg I (#JAL–1121–AVT40). A. Tibia I and metatarsus I, prolateral view. B. Apical tibia I and metatarsus I showing the clasper field, ventral view. 19. Male bulbs from the three populations examined in this study. A. Male from the Gredos sample (#MNCN 20.02/19859). B. Distal embolus seen at higher magnification; note the presence of two small denticles on the convex side. C. Male from the Daimiel sample (#EM–2126–2). D. Smooth distal embolus at higher magnification. E. Male from the Alcolea-Córdoba sample (#CCPP–0029–2). F. Distal embolus at higher magnification; arrows point to two tiny, hardly visible denticles; the triangle marks a small protuberance in the distal tip of the embolus, seen in some males. 20. Some teratological specimens found in our material. A. Male showing an unusually narrow sternum (#CCPP–0028). B. Atypical double spur on left tibia I (#RTJ–7). C. Posterior lung plates abnormally stained dark brown. Scale bars = 1.00 mm (16A, 18A–B, 20A–B); 0.50 mm (17A–J, 20C); 0.25 mm (19A, C, E); 0.10 mm (19 B, D, F). // **Fig. 16–20.** Macho de *Iberesia castillana* (continuación). 16. Palpo derecho, vista retrolateral (#MNCN 20.02/19859). 17. Diferentes alineamientos de espinas del rastrillo dorsoapical de la tibia del palpo, ordenados de más frecuentes (A–C) a menos frecuentes (G–J); vista ligeramente prodorsal (no se muestran todos los alineamientos observados). A. 3+1+1 (#JAL–1120–AVT40). B. 3+0+1 (#JAL–1121–AVT40). C. 3+2+1 (#JAL–1120–AVT40). D. 2+0+1 (#CCPP–0029–1). E. 4+1+1 (#JAL–1258–AVT40). F. 3+1+1+1 (#CCPP–0029–2). G. 3+2+1+1 (#MIG–056f). H. 4+2+1 (#MIG–056c). I. 1+0+1 (#JAL–1122–AVT40). J. 1+0+0 (#MIG–056f). 18. Cláspero, pata I izquierda (#JAL–1121–AVT40). A. Tibia I y metatarso I, vista prolateral. B. Extremo apical de la tibia I, y metatarso I, vista ventral. 19. Bulbos de machos de las tres poblaciones estudiadas en este trabajo. A. Macho de la muestra de Gredos (#MNCN 20.02/19859). B. Extremo distal del émbolo visto a mayor aumento; nótese la presencia de dos pequeños dientecillos en el lado convexo. C. Macho de la muestra de Daimiel (#EM–2126–2). D. Extremo distal liso del émbolo a mayor aumento. E. Macho de la muestra de Alcolea-Córdoba (#CCPP–0029–2). F. Émbolo distal a mayor aumento; las flechas apuntan a dos minúsculos dentículos difíciles de apreciar; el triángulo indica una pequeña protuberancia presente en la punta del émbolo de algunos machos. 20. Algunos ejemplares teratológicos encontrados en el material examinado. A. Macho con un esternón inusualmente estrecho (#CCPP–0028). B. Doble espolón atípico en la tibia I izquierda (#RTJ–7). C. Placas pulmonares posteriores anormalmente teñidas de marrón oscuro. Barras de escala = 1.00 mm (16A, 18A–B, 20A–B); 0.50 mm (17A–J, 20C); 0.25 mm (19A, C, E); 0.10 mm (19B, D, F).


16
17
A
B
C
D
E
F
G
H
I
J
18
A
B
19
A
B
C
D
E
F
20
A
B
C

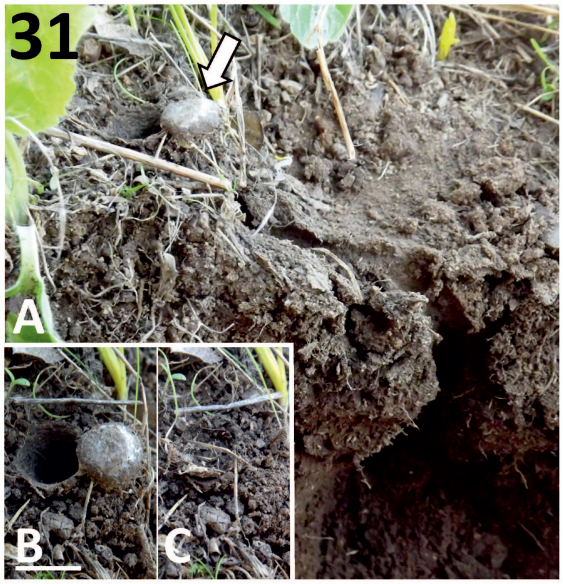
► **Fig. 21–29.** Female of *Iberesia castillana*. 21. Habitus and coloration of living females. A. Female from the Gredos sample (#MNCN 20.02/19861). B. Female from the Alcolea-Córdoba sample (#CCPP–0084). 22 Habitus and coloration of preserved females. A. Female from the Gredos sample (#MNCN 20.02/19861). B. Gravid female from the Alcolea-Córdoba sample (#CCPP–0056). 23. Carapace, lateral view (#CCPP–0056). 24. Eye group. A. Female from Gredos sample (#MNCN 20.02/19861). B. Female from the Alcolea-Córdoba sample (#CCPP–0056). 25. Habitus, ventral view (#MNCN 20.02/19861). 26. Sternum, labium, and maxillae; note the barely perceptible sigilla close to the sternal margin (#MNCN 20.02/19861). 27. Some details of maxillae and chelicerae; ventrolateral view: blunt conical cuspules, row of six unequal cheliceral teeth, group of mesobasal denticles in the cheliceral furrow, finely notched fang keel (#MNCN 20.02/19861). 28. Spinnerets (#MIG–010b). A. PLS fully extended, ventral view. B. Caudal view of the distal segment of spinnerets, each showing a central group of three macro-spigots surrounded by sparse rings of smaller spigots. 29. Spermathecae. A–C: females from the Gredos sample. A. Female #JAL–1293–AVT40. B. Female #MNCN 20.02/19861. C. Female #JAL–1281–AVT40. D–F: females from the Alcolea-Córdoba sample. D. Female #CCPP–0056. E. Female #MIG–037. F. Female #MIG–012b. Scale bars = 2.00 mm (22A–B, 25); 1.00 mm (23, 26, 27); 0.50 mm (28A); 0.25 mm (24A–B); 0.15 mm (28B, 29A–F). // **Fig. 21–29**. Hembra de *Iberesia castillana*. 21. Habitus y coloración de ejemplares vivos. A. Hembra de la muestra de Gredos (#MNCN 20.02/19861). B. Hembra de la muestra de Alcolea-Córdoba (#CCPP–0084). 22 Habitus y coloración de ejemplares conservados. A. Hembra de la muestra de Gredos (#MNCN 20.02/19861). B. Hembra grávida de la muestra de Alcolea-Córdoba (#CCPP–0056). 23. Caparazón, vista lateral (#CCPP–0056). 24. Formación ocular. A. Hembra de la muestra de Gredos (#MNCN 20.02/19861). B. Hembra de la muestra de Alcolea-Córdoba (#CCPP–0056). 25 Habitus, vista ventral (#MNCN 20.02/19861). 26. Esternón, labio y maxilas; se observan las sigilas, apenas visibles, próximas al margen del esternón (#MNCN 20.02/19861). 27. Detalle de las maxilas y quelíceros, vista ventrolateral: cúspulas cónicas romas, fila de seis dientes quelicerales desiguales, grupo de dentículos mesobasales en el surco queliceral, filo del colmillo finamente mellado (#MNCN 20.02/19861). 28. Hileras (#MIG–010b). A. Hileras posteriores laterales completamente extendidas, vista ventral. B. Vista caudal del segmento distal de las hileras que muestra un grupo central de tres macrofúsulas, rodeadas de anillos poco densos de fúsulas de menor tamaño. 29. Espermatecas. A–C: hembras de la muestra de Gredos. A. Hembra #JAL–1293–AVT40. B. Hembra #MNCN 20.02/19861. C. Hembra #JAL–1281–AVT40. D–F: hembras de la muestra de Alcolea-Córdoba. D. Hembra #CCPP–0056. E. Hembra #MIG–037. F. Hembra #MIG–012b. Barras de escala = 2,00 mm (22A–B, 18); 1,00 mm (23, 26, 27); 0,50 mm (28A); 0,25 mm (24A–B); 0,15 mm (28B, 29A–F).

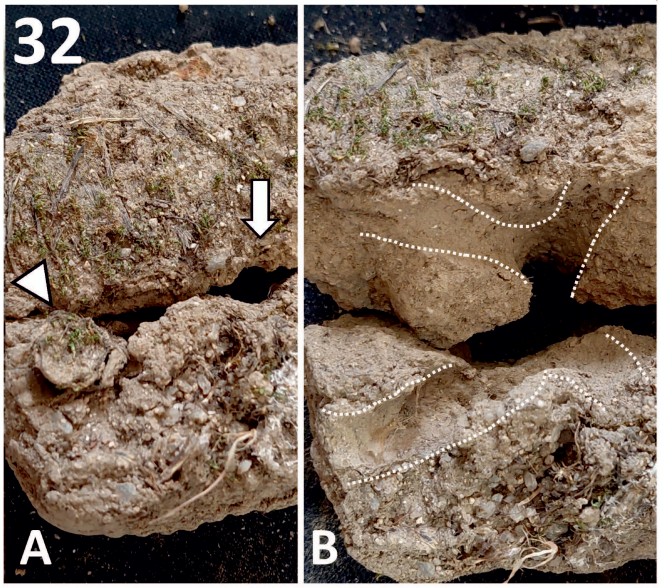

21
A
B
22
A
B
23
24
A
B
25
26
27
28
A
B
29
A
B
C
D
E
F

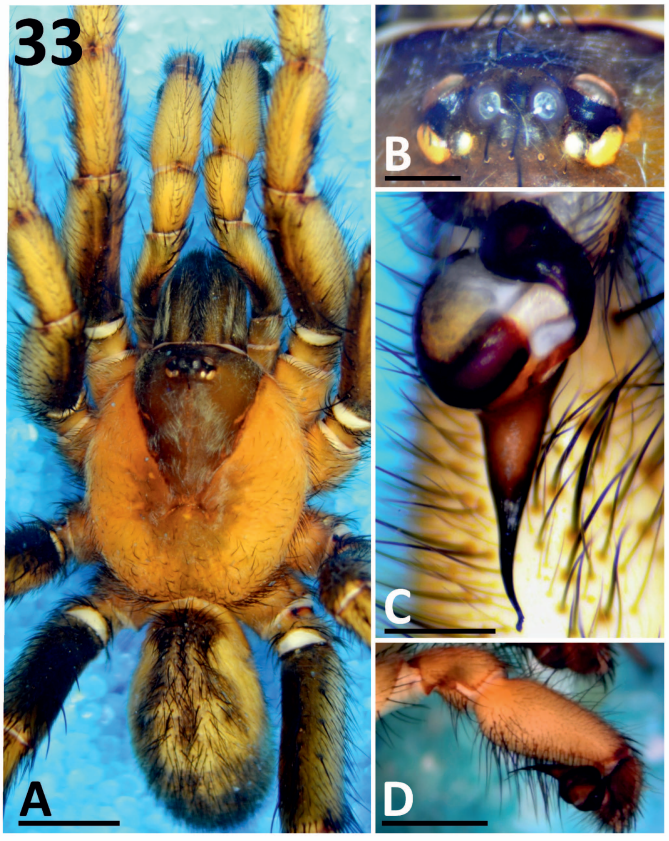
► **Fig. 30–32.** Habitat and nest of *Iberesia castillana*. 30. Panoramic of a *dehesa* in the Alcolea area (Córdoba province), a characteristic habitat of this species. 31. Nest of *I. castillana* (#CCPP–0084). A. Excavated burrow showing tube with infrequent broken trajectory; arrow points to open trapdoor. B–C: Burrow entrance. B. Trapdoor open. C. Trapdoor closed. 32. Entrance of a nest of *I. castillana* unusually branched near the opening (#MNCN 20.02/19861). A. The arrow points to the main entrance, the triangle to the secondary entrance. B. Upper part of the same nest open in the sagittal plane; the dotted lines indicate the two branches of the burrow; the lateral gallery is formed from the lateral widening under the main entrance. Similar lateral openings have been found in some nemesiid and ctenizids that build unbranched nests when the main entrance is blocked, both in captivity and in the wild (Calvo, pers. observation). Scale bar = 5.00 mm. // **Fig. 30–32.** Hábitat y nido de *Iberesia castillana*. 30. Panorámica de una dehesa en la zona de Alcolea (provincia de Córdoba), hábitat característico de esta especie. 31. Nido de *I. castillana* (#CCPP–0084). A. Madriguera excavada que muestra la galería con una trayectoria quebrada poco habitual; la flecha señala la trampilla abierta. B–C: Entrada de la madriguera. B. Trampilla abierta. C. Trampilla cerrada. 32. Entrada de un nido de *I. castillana* ramificada cerca de la abertura de modo inusual (#MNCN 20.02/19861). A. La flecha indica la posición de la entrada principal, el triángulo, el de la entrada secundaria. B. Parte alta del mismo nido seccionado en el plano sagital; las líneas de puntos indican la trayectoria de las galerías principal y accesoria de la madriguera; la galería accesoria fue excavada a partir del ensanchamiento lateral bajo la entrada principal. Se han hallado nidos con aberturas laterales similares en algunos nemésidos y ctenícidos que excavan nidos no ramificados cuando la entrada principal está bloqueada, tanto en cautividad como en la naturaleza (Calvo, observación personal). Escala = 5,00 mm.

► **Fig. 33–34.** Comparison between the male of *Iberesia machadoi* and *Iberesia castillana* holotype. 33. Male of *Iberesia machadoi* (#M20171013-1). A. Dorsal habitus. B. Eye formation. C. Palpal bulb. D. Palpal tibia. 34. Holotype of *Iberesia castillana* (#MNHN AR4341). A. Dorsal habitus. B. Eye formation. C. Palpal bulb; note than the tip of the embolus is broken; the inset shows the same bulb drawn before it was damaged (Decae & Cardoso, 2005). D. Palpal tibia. Photographs from the holotype of *I. castillana* courtesy of Ms. Leguin, from the MNHN. Scale bars = 2.00 mm (33A, D; 34A, D), 0.50 mm (33B, C; 34B, C); pairs of photographs with the same letter adjusted to the same scale. // **Fig. 33–34.** Comparación entre el macho de *Iberesia machadoi* y el holotipo de *Iberesia castillana*. 33. Macho de Iberesia machadoi (#M20171013-1). A. Habitus dorsal. B. Formación ocular. C. Bulbo. D. Tibia del palpo. 34. Holotipo de *Iberesia castillana* (#MNHN AR4341). A. Habitus dorsal. B. Formación ocular. C. Bulbo; nótese que la punta del émbolo está rota; el recuadro muestra un dibujo del mismo bulbo hecho antes de que el émbolo resultase dañado (Decae & Cardoso, 2005). D. Tibia del palpo. Las fotografías del holotipo de *I. castillana* son cortesía de la Srta. Leguin, del MNHN. Escala = 2,00 mm (33A, D; 34A, D), 0,50 mm (33B–C; 34B–C); pares de fotografías con la misma letra ajustadas a la misma escala.


30


31
A
B
C


32
A
B


33
A
B
C
D

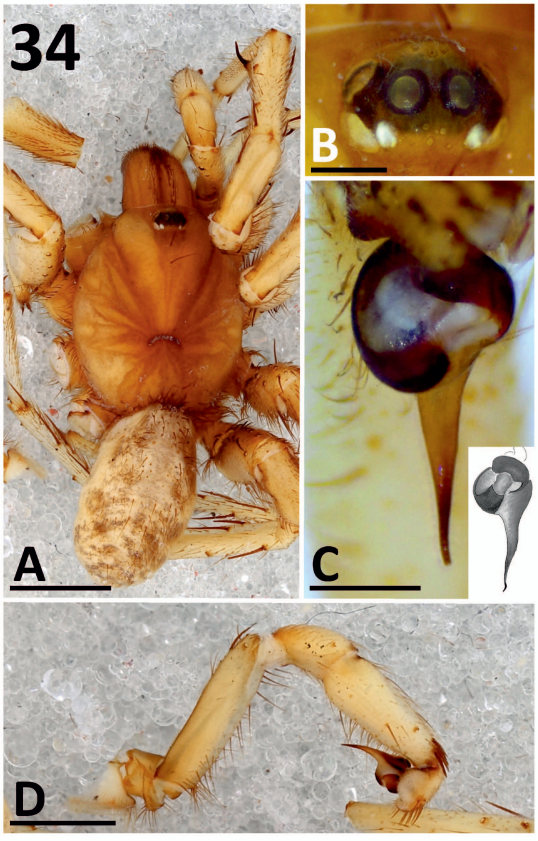

34
A
B
C
D

Table I. Material examined in this study. // **Tabla I.** Material examinado en este estudio.

(1) Female collected from her burrow with two spiderlings. (*) Material deposited at the MNCN: JAL–1119–AVT40 = MNCN 20.02/19859; JAL–1125–AVT40 = MNCN 20.02/19860; JAL–1280–AVT40 = MNCN 20.02/19861. (**) Material deposited at the MNHN: JAL–1133–AVT41 = MNHN AR16177; JAL–1250–AVT40 = MNHN AR16178. // (1) Hembra recogida en su nido con dos crías. (*) Material depositado en el MNCN: JAL–1119–AVT40 = MNCN 20.02/19859; JAL–1125–AVT40 = MNCN 20.02/19860; JAL–1280–AVT40 = MNCN 20.02/19861. (**) Material depositado en el MNHN: JAL–1133–AVT41 = MNHN AR16177; JAL–1250–AVT40 = MNHN AR16178.

Reference	Collection	Sex	State	Coll. date	Collection Method	Leg.	Species	Locality	Province	Longitude	Latitude	Altitude
Sample from Sierra de Gredos (Ávila)												
JAL-1119-AVT40 (*)	JAL	♂	Adult	16 Nov. 2019	pitfall trap	J.A. Luis	*I. castillana*	Arenas de San Pedro	Ávila	40.156444	-5.070970	395
JAL-1120-AVT40	JAL	♂	Adult	16 Nov. 2019	pitfall trap	J.A. Luis	*I. castillana*	Arenas de San Pedro	Ávila	40.156444	-5.070970	395
JAL-1121-AVT40	JAL	♂	Adult	16 Nov. 2019	pitfall trap	J.A. Luis	*I. castillana*	Arenas de San Pedro	Ávila	40.156444	-5.070970	395
JAL-1122-AVT40	JAL	♂	Adult	16 Nov. 2019	pitfall trap	J.A. Luis	*I. castillana*	Arenas de San Pedro	Ávila	40.156444	-5.070970	395
JAL-1123-AVT40	JAL	♂	Adult	16 Nov. 2019	pitfall trap	J.A. Luis	*I. castillana*	Arenas de San Pedro	Ávila	40.156444	-5.070970	395
JAL-1124-AVT40	JAL	♂	Adult	16 Nov. 2019	pitfall trap	J.A. Luis	*I. castillana*	Arenas de San Pedro	Ávila	40.156444	-5.070970	395
JAL-1125-AVT40 (*)	JAL	♂	Adult	16 Nov. 2019	pitfall trap	J.A. Luis	*I. castillana*	Arenas de San Pedro	Ávila	40.156444	-5.070970	395
JAL-1126-AVT40	JAL	♂	Adult	16 Nov. 2019	pitfall trap	J.A. Luis	*I. castillana*	Arenas de San Pedro	Ávila	40.156444	-5.070970	395
JAL-1127-AVT40	JAL	♂	Adult	16 Nov. 2019	pitfall trap	J.A. Luis	*I. castillana*	Arenas de San Pedro	Ávila	40.156444	-5.070970	395
JAL-1128-AVT40	JAL	♂	Adult	16 Nov. 2019	pitfall trap	J.A. Luis	*I. castillana*	Arenas de San Pedro	Ávila	40.156444	-5.070970	395
JAL-1133-AVT41(**)	JAL	♂	Adult	16 Nov. 2019	pitfall trap	J.A. Luis	*I. castillana*	Arenas de San Pedro	Ávila	40.156468	-5.071063	394
JAL-1134-AVT41	JAL	♂	Adult	16 Nov. 2019	pitfall trap	J.A. Luis	*I. castillana*	Arenas de San Pedro	Ávila	40.156468	-5.071063	394
JAL-1136-AVT41	JAL	♂	Adult	2 Nov. 2019	pitfall trap	M. Calvo	*I. castillana*	Arenas de San Pedro	Ávila	40.156468	-5.071063	394
JAL-1243-AVT30	JAL	♂	Adult	7 Dec. 2019	pitfall trap	J.A. Luis	*I. castillana*	Mombeltrán	Ávila	40.244277	-5.025109	526
JAL-1245-AVT40	JAL	♂	Adult	7 Dec. 2019	pitfall trap	J.A. Luis	*I. castillana*	Arenas de San Pedro	Ávila	40.156444	-5.070970	395
JAL-1246-AVT40	JAL	♂	Adult	7 Dec. 2019	pitfall trap	J.A. Luis	*I. castillana*	Arenas de San Pedro	Ávila	40.156444	-5.070970	395
JAL-1247-AVT40	JAL	♂	Adult	7 Dec. 2019	pitfall trap	J.A. Luis	*I. castillana*	Arenas de San Pedro	Ávila	40.156444	-5.070970	395
JAL-1248-AVT40	JAL	♂	Adult	7 Dec. 2019	pitfall trap	J.A. Luis	*I. castillana*	Arenas de San Pedro	Ávila	40.156444	-5.070970	395
JAL-1249-AVT40	JAL	♂	Adult	7 Dec. 2019	pitfall trap	J.A. Luis	*I. castillana*	Arenas de San Pedro	Ávila	40.156444	-5.070970	395
JAL-1250-AVT40 (**)	JAL	♀	Adult	7 Dec. 2019	pitfall trap	J.A. Luis	*I. castillana*	Arenas de San Pedro	Ávila	40.156444	-5.070970	395
JAL-1251-AVT40	JAL	♂	Adult	7 Dec. 2019	pitfall trap	J.A. Luis	*I. castillana*	Arenas de San Pedro	Ávila	40.156444	-5.070970	395
JAL-1252-AVT40	JAL	♂	Adult	7 Dec. 2019	pitfall trap	J.A. Luis	*I. castillana*	Arenas de San Pedro	Ávila	40.156444	-5.070970	395
JAL-1253-AVT40	JAL	♂	Adult	7 Dec. 2019	pitfall trap	J.A. Luis	*I. castillana*	Arenas de San Pedro	Ávila	40.156444	-5.070970	395
JAL-1254-AVT40	JAL	♂	Adult	7 Dec. 2019	pitfall trap	J.A. Luis	*I. castillana*	Arenas de San Pedro	Ávila	40.156444	-5.070970	395
JAL-1255-AVT40	JAL	♂	Adult	7 Dec. 2019	pitfall trap	J.A. Luis	*I. castillana*	Arenas de San Pedro	Ávila	40.156444	-5.070970	395
JAL-1256-AVT40	JAL	♂	Adult	7 Dec. 2019	pitfall trap	J.A. Luis	*I. castillana*	Arenas de San Pedro	Ávila	40.156444	-5.070970	395
JAL-1257-AVT40	JAL	♂	Adult	7 Dec. 2019	pitfall trap	J.A. Luis	*I. castillana*	Arenas de San Pedro	Ávila	40.156444	-5.070970	395
JAL-1258-AVT40	JAL	♂	Adult	7 Dec. 2019	pitfall trap	J.A. Luis	*I. castillana*	Arenas de San Pedro	Ávila	40.156444	-5.070970	395
JAL-1259-AVT40	JAL	♀	Adult	7 Dec. 2019	pitfall trap	J.A. Luis	*I. castillana*	Arenas de San Pedro	Ávila	40.156444	-5.070970	395
JAL-1278	JAL	♀	Adult	28 Dec. 2019	burrow excavation	S. Luis	*I. castillana*	Arenas de San Pedro	Ávila	40.156444	-5.070040	395
JAL-1279	JAL	♀	Adult	28 Dec. 2019	burrow excavation	M. Calvo	*I. castillana*	Arenas de San Pedro	Ávila	40.155313	-5.071384	392
JAL-1280-AVT40 (*)	JAL	♀	Adult	28 Dec. 2019	pitfall trap	J.A. Luis	*I. castillana*	Arenas de San Pedro	Ávila	40.156444	-5.070970	395
JAL-1281	JAL	♀	Adult	28 Dec. 2019	burrow excavation	M. Calvo	*I. castillana*	Arenas de San Pedro	Ávila	40.155707	-5.070358	399
JAL-1293-AVT40	JAL	♀	Adult	28 Dec. 2019	pitfall trap	J.A. Luis	*I. castillana*	Arenas de San Pedro	Ávila	40.156444	-5.070970	395
JAL-1289-AVT40	JAL	♂	Adult	28 Dec. 2019	pitfall trap	M. Calvo	*I. castillana*	Arenas de San Pedro	Ávila	40.156444	-5.070970	395
JAL-1291-AVT40	JAL	♂	Adult	28 Dec. 2019	pitfall trap	J.A. Luis	*I. castillana*	Arenas de San Pedro	Ávila	40.156444	-5.070970	395
JAL-1292-AVT40	JAL	♂	Adult	28 Dec. 2019	pitfall trap	J.A. Luis	*I. castillana*	Arenas de San Pedro	Ávila	40.156444	-5.070970	395
JAL-1352	JAL	♂	Adult	11 Jan. 2020	found dead	A. Narro	*I. castillana*	El Tiemblo	Ávila	40.422056	-4.506980	655
Sample from Parque Nacional Las Tablas de Daimiel & Fuencaliente (Ciudad Real)												
EM-53-1	EM	♂	Adult	11 Dec. 2014	pitfall trap	E. Morano	*I. castillana*	P. N. La Tablas de Daimiel	Ciudad Real	39.167191	-3.682035	610
EM-53-2	EM	♂	Adult	11 Dec. 2014	pitfall trap	E. Morano	*I. castillana*	P. N. La Tablas de Daimiel	Ciudad Real	39.167191	-3.682035	610
EM-204	EM	♂	Adult	15 Jan. 2015	pitfall trap	E. Morano	*I. castillana*	P. N. La Tablas de Daimiel	Ciudad Real	39.137983	-3.704344	609
EM-2126-1	EM	♂	Adult	12 Nov. 2015	pitfall trap	E. Morano	*I. castillana*	P. N. La Tablas de Daimiel	Ciudad Real	39.167191	-3.682035	610
EM-2126-2	EM	♂	Adult	12 Nov. 2015	pitfall trap	E. Morano	*I. castillana*	P. N. La Tablas de Daimiel	Ciudad Real	39.167191	-3.682035	610
EM-2126-3	EM	♂	Adult	12 Nov. 2015	pitfall trap	E. Morano	*I. castillana*	P. N. La Tablas de Daimiel	Ciudad Real	39.167191	-3.682035	610
EM-2126-4	EM	♂	Juvenile	12 Nov. 2015	pitfall trap	E. Morano	*I. castillana*	P. N. La Tablas de Daimiel	Ciudad Real	39.167191	-3.682035	610
EM-2191	EM	♂	Adult	12 Nov. 2015	pitfall trap	E. Morano	*I. castillana*	P. N. La Tablas de Daimiel	Ciudad Real	39.137983	-3.704344	609

Reference	Collection	Sex	State	Coll. date	Collection Method	Leg.	Species	Locality	Province	Longitude	Latitude	Altitude
CCPP-0081	CPP	♂	Adult	30 Sep 2020	Manual collection	G. Rodríguez	*I. castillana*	Fuencaliente	Ciudad Real	37.440110	-4.318380	742
Sample from Alcolea & Córdoba												
JAL-804	JAL	♂	Adult	18 Jan. 2018	Manual collection	C. Pertegal	*I. castillana*	Alcolea	Córdoba	37.955444	-4.721747	379
JAL-805	JAL	♂	Adult	18 Jan. 2018	Manual collection	C. Pertegal	*I. castillana*	Alcolea	Córdoba	37.955444	-4.721747	379
CCPP-0028	CPP	♂	Adult	unknown	Manual collection	C. Pertegal	*I. castillana*	unknown	Córdoba		unknown	
CCPP-0029-1	CPP	♂	Adult	13 Jan. 2019	Manual collection	C. Pertegal	*I. castillana*	Alcolea	Córdoba	37.945200	-4.715725	193
CCPP-0029-2	CPP	♂	Adult	13 Jan. 2019	Manual collection	C. Pertegal	*I. castillana*	Alcolea	Córdoba	37.945200	-4.715725	193
CCPP-0029-3	CPP	♂	Adult	13 Jan. 2019	Manual collection	C. Pertegal	*I. castillana*	Alcolea	Córdoba	37.945200	-4.715725	193
CCPP-0056	CPP	♀	Adult	2018	burrow excavation	C. Pertegal	*I. castillana*	Alcolea	Córdoba	37.945200	-4.715725	193
CCPP-0079	CPP	♀	Adult	30 Sep 2020	burrow excavation	C. Pertegal	*I. castillana*	Alcolea	Córdoba	37.945116	-4.702468	198
CCPP-0082	CPP	♀	Adult	25 Oct 2020	burrow excavation	C. Pertegal	*I. castillana*	Alcolea	Córdoba	37.941837	-4.692095	178
CCPP-0083	CPP	♀	Adult	25 Oct 2020	burrow excavation	C. Pertegal	*I. castillana*	Alcolea	Córdoba	37.941837	-4.692095	178
CCPP-0084	CPP	♀	Adult	1 Nov 2020	burrow excavation	C. Pertegal	*I. castillana*	Alcolea	Córdoba	37.943681	-4.693726	184
CCPP-0085	CPP	♀	Adult	1 Nov 2020	burrow excavation	C. Pertegal	*I. castillana*	Alcolea	Córdoba	37.944984	-4.693018	168
CCPP-0086	CPP	♀	Adult	1 Nov 2020	burrow excavation	C. Pertegal	*I. castillana*	Alcolea	Córdoba	37.944984	-4.693018	168
CCPP-0090	CPP	♀	Adult	22 Nov 2020	burrow excavation	C. Pertegal	*I. castillana*	El Higuerón	Córdoba	37.852979	-4.823823	104
CCPP-0091	CPP	♀	Adult	22 Nov 2020	burrow excavation	C. Pertegal	*I. castillana*	El Higuerón	Córdoba	37.852979	-4.823823	104
CCPP-0092	CPP	♀	Adult	22 Nov 2020	burrow excavation	C. Pertegal	*I. castillana*	El Higuerón	Córdoba	37.852979	-4.823823	104
CCPP-0093	CPP	♀	Adult	22 Nov 2020	burrow excavation	C. Pertegal	*I. castillana*	El Higuerón	Córdoba	37.852979	-4.823823	104
MIG-002a	UCO	♀	Adult	9 Sep 2018	burrow excavation	C. Pertegal	*I. castillana*	Alcolea	Córdoba	37.943878	-4.694289	183
MIG-010a (1)	UCO	♀	Adult	16 Sep 2018	burrow excavation	C. Pertegal	*I. castillana*	Alcolea	Córdoba	37.943878	-4.694289	183
MIG-010b	UCO	♀	Adult	16 Sep 2018	burrow excavation	C. Pertegal	*I. castillana*	Alcolea	Córdoba	37.943878	-4.694289	183
MIG-012a	UCO	♀	Adult	22 Apr 2018	burrow excavation	C. Pertegal	*I. castillana*	Alcolea	Córdoba	37.943878	-4.694289	183
MIG-012b	UCO	♀	Adult	22 Apr 2018	burrow excavation	C. Pertegal	*I. castillana*	Alcolea	Córdoba	37.943878	-4.694289	183
MIG-016	UCO	♂	Adult	18 Dec 2017	Manual collection	C. Pertegal	*I. castillana*	Córdoba	Córdoba	37.908839	-4.721747	198
MIG-018a	UCO	♂	Adult	9 Oct 2017	Manual collection	C. Pertegal	*I. castillana*	Córdoba	Córdoba	37.907700	-4.758299	116
MIG-018b	UCO	♂	Adult	9 Oct 2017	burrow excavation	C. Pertegal	*I. castillana*	Córdoba	Córdoba	37.907700	-4.758299	116
MIG-019a	UCO	♀	Adult	18 Jan 2018	burrow excavation	C. Pertegal	*I. castillana*	Alcolea	Córdoba	37.943878	-4.694289	183
MIG-019b	UCO	♂	Adult	18 Jan 2018	Manual collection	C. Pertegal	*I. castillana*	Alcolea	Córdoba	37.943878	-4.694289	183
MIG-019c	UCO	♂	Adult	18 Jan 2018	Manual collection	C. Pertegal	*I. castillana*	Alcolea	Córdoba	37.943878	-4.694289	183
MIG-037	UCO	♀	Adult	22 Apr 2018	burrow excavation	C. Pertegal	*I. castillana*	Alcolea	Córdoba	37.943878	-4.694289	183
MIG-056a	UCO	♂	Adult	29 Nov 2018	Manual collection	C. Pertegal	*I. castillana*	Alcolea	Córdoba	37.935186	-4.808183	372
MIG-056b	UCO	♂	Adult	29 Nov 2018	Manual collection	C. Pertegal	*I. castillana*	Alcolea	Córdoba	37.935186	-4.808183	372
MIG-056c	UCO	♂	Adult	29 Nov 2018	Manual collection	C. Pertegal	*I. castillana*	Alcolea	Córdoba	37.935186	-4.808183	372
MIG-056d	UCO	♂	Adult	29 Nov 2018	Manual collection	C. Pertegal	*I. castillana*	Alcolea	Córdoba	37.935186	-4.808183	372
MIG-056e	UCO	♂	Adult	29 Nov 2018	Manual collection	C. Pertegal	*I. castillana*	Alcolea	Córdoba	37.935186	-4.808183	372
MIG-056f	UCO	♂	Adult	29 Nov 2018	Manual collection	C. Pertegal	*I. castillana*	Alcolea	Córdoba	37.935186	-4.808183	372
MIG-057	UCO	♂	Adult	1 Dec 2018	Manual collection	C. Pertegal	*I. castillana*	Alcolea	Córdoba	37.907700	-4.758299	116
MIG-066	UCO	♀	Adult	15 Mar 2019	burrow excavation	C. Pertegal	*I. castillana*	Alcolea	Córdoba	37.943878	-4.694289	183
RTJ-7	RTJ	♂	Adult	3 Dec 1988	Manual collection	R. Tamajón	*I. castillana*	Córdoba	Córdoba	37.907337	-4.721747	127
RTJ-14	RTJ	♂	Adult	3 Dec 1988	Manual collection	R. Tamajón	*I. castillana*	Córdoba	Córdoba	37.907337	-4.721747	127
RTJ-15	RTJ	♂	Adult	3 Dec 1988	Manual collection	R. Tamajón	*I. castillana*	Córdoba	Córdoba	37.907337	-4.721747	127
Other material studied												
JAL-1271	JAL	♀	Adult	20 Dec 2019	burrow excavation	M. Calvo	*I. arturica*	El Palmar	Murcia	37.914486	-1.176083	149
JAL-1353	JAL	♀	Adult	8 Mar 2020	burrow excavation	A. Narro	*I. valdemoriana*	Rosas	Madrid	40.427074	-3.592629	666
JAL-1359	JAL	♂	Adult	26 Aug 2020	pitfall trap	M. Calvo	*I. arturica*	El Palmar	Murcia	37.914854	-1.177532	156
CCPP-0030	CPP	♂	Adult	7 Nov 2019	Manual collection	C. Pertegal	*I. machadoi*	Puebla de Sancho Pérez	Badajoz	38.397824	-6.405025	506
EM-1253	EM	♂	Adult	unknown	pitfall trap	E. Morano	*I. valdemoriana*	unknown	Toledo		unknown	
EM-1254	EM	♂	Adult	unknown	pitfall trap	E. Morano	*I. valdemoriana*	unknown	Toledo		unknown	
EM-1255	EM	♂	Adult	unknown	pitfall trap	E. Morano	*I. valdemoriana*	unknown	Toledo		unknown	
JABA-304	JABA	♂	Adult	13 Oct 2017	pitfall trap	JA. Barrientos	*Nemesia athiasi*	Plasencia	Cáceres	40.066364	-6.081613	225
M20171012-1	MCG	♀	Adult	12 Oct 2017	burrow excavation	M. Calvo	*I. machadoi*	Villarreal de San Carlos	Cáceres	39.848136	-6.025765	299
M20171013-1	MCG	♂	Adult	13 Oct 2017	burrow excavation	M. Calvo	*I. machadoi*	Plasencia	Cáceres	40.067590	-6.080636	560
M20171013-2	MCG	♀	Adult	13 Oct 2017	burrow excavation	M. Calvo	*I. machadoi*	Plasencia	Cáceres	40.147539	-5.878879	420
M20171013-3	MCG	♀	Adult	13 Oct 2017	burrow excavation	M. Calvo	*I. machadoi*	Plasencia	Cáceres	40.147531	-5.878889	429